Ancient TL

www.ancienttl.org · ISSN: 2693-0935

Issue 24(2) - December 2006
https://doi.org/10.26034/la.atl.v24.i2

Use of magnetic separation for purifying quartz for luminescence dating

Naomi Porat

Geological Survey of Israel, 30 Malkhe Israel St., Jerusalem 95501, Israel
(e-mail: naomi.porat@gsi.gov.il)

(Received 6 November 2006; in final form 14 November 2006)

Introduction

The increased use of the single aliquot regenerative (SAR) dose protocol and its current acceptance as the preferred protocol for dating quartz calls for efficient methods for purifying quartz. Common components of the sediment that need to be removed are salts, clays, carbonates, organic matter, heavy minerals and feldspars. Salts are usually water soluble; clays can be removed by sieving or decanting; carbonates are dissolved by 5-10% HCl; and organic matter is oxidized by concentrated peroxide or bleach.

Removing heavy minerals and feldspars is normally the most time consuming part of the procedure. Commonly, heavy minerals, feldspars and other contaminant minerals are removed by a 2-step density separation, using heavy liquids with densities that are slightly heavier and slightly lighter than quartz (Wintle, 1997). As it is imperative that the purified quartz contains no measurable feldspar, concentrated (40-48%) hydrofluoric acid (HF) is typically used to dissolve the remaining feldspars and at the same time etch the quartz.

An alternative method for removing heavy minerals and most feldspars is magnetic separation. Whilst this is not a new procedure (Rosenblum, 1958), the use of it within luminescence is currently not common. Aitken (1985; p.18) mentions it as one of the many techniques used for mineral separation, and in the past it was used in the Research Laboratory for Archaeology and the History of Art, Oxford (Fleming, 1966). This paper aims to provide a description of the procedure.

The advantages of magnetic separation are effectiveness and simplicity. The modern magnetic separators are stable and the results reproducible. The non-magnetic fraction remaining after separation consists of almost pure quartz and can be etched with relatively small volumes of HF, thus saving time, chemicals and heavy liquids.

The need for a different method for mineral separation in the luminescence dating laboratory at the Geological Survey of Israel (GSI) arose when attempting to extract quartz from sediments of alluvial fans in hyperarid regions. Besides quartz and feldspars, these poorly sorted sediments contained large amounts of very angular sand-sized chert. These chert grains could not be dated by OSL as, first, they were mostly not allochthonous but formed within the sediment by shattering and disintegration of chert pebbles due to action of salts, and had thus not seen sunlight; and second, due to their opacity they do not bleach during transport. Therefore it was crucial to remove the chert for successful dating.

The chert could not be separated from the quartz by the physical or chemical methods commonly used at the time in the laboratory, such as density separation or selective dissolution, because the density of chert is close to that of quartz, and it is only marginally more soluble than quartz in HF. Fortuitously, magnetic separation using a Frantz LB1 with a high current on the magnet proved suitable for removing the chert as well as most feldspars, insoluble dolomite and the majority of heavy minerals. Subsequent heavy liquid separation at a density of 2.7 g/cm^3 showed that only several grains of heavy mineral remained, mostly apatite and fluorite. Zircon, a luminescent mineral, is very rare in sediments and is highly unlikely to remain after magnetic separation.

Magnetic separation is a common physical method used for separating minerals with different magnetic properties. In industry it is used to concentrate ferromagnetic and paramagnetic ore minerals (e.g. Augusto and Martins, 1999). In Earth Sciences it is used for extracting diamagnetic mineral fractions from igneous and metamorphic rocks for dating or for geochemical analyses (e.g. Kolodner et al., 2006).

Equipment description

Magnetic separators used in Earth Science laboratories comprise an electromagnet, a feeder, and a sloping and tilting chute that pass the grains by the magnet (Figure 1). The grains fall from the feeder and move along the chute due to its vibration. As each grain runs by the magnet it is either attracted to the magnet or it falls to the sloping side of the chute. A split in the chute separates the more magnetic from the less magnetic grains, and each are collected in separate, designated boxes. By adjusting the current on the magnet using guides from published tables (Rosenblum, 1958) and trial and error, almost any two minerals can be separated. Adjusting the slope and tilt is useful for different grain sizes and shapes.

Magnetic separation is now used at the GSI laboratory as part of the routine mineral separation protocol. It follows sieving and dissolution of carbonates. The sample needs to be washed of fines (<40 µm) and dry. The Franz magnetic separator is situated in the dark laboratory and separation is carried out under the required subdued orange-red light. A small red pin-light is used to check the grain flow from the feeder onto the chute.

The feeder may contain up to 100 g, but most samples for OSL dating are much smaller. Sample flow can be as high as 10 g/min, still with effective separation. However a more practical flow rate is about 2 g/min, which would take about 10 minutes to separate a characteristic sample weighing 20 g. There is essentially no sample loss and even very small samples (a few hundred mg) can easily be separated and retrieved using low flow rates.

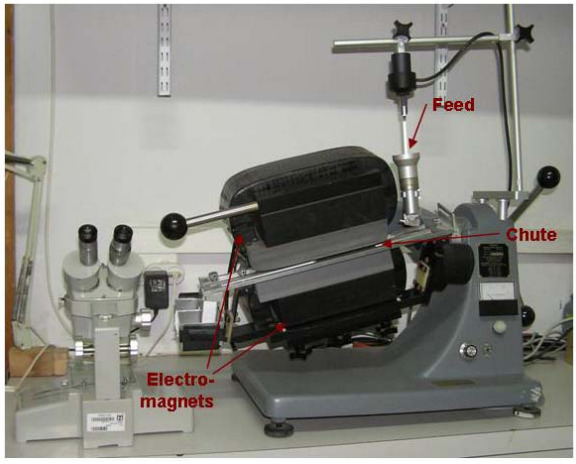

Figure 1: *The Frantz Magnetic Barrier Laboratory Separator Model LB-1 at the GSI.*

So far, separation has proved to be efficient for a large range of grain sizes, from 64 µm to 350 µm, and the resulting quartz is very clean (Figure 2). Over the years, quartz has been extracted in this way from a variety of soils (Terra Rossa, basaltic soils, rendsina), desert loess, and fluvial and aeolian sediments.

Effective separation is judged visually by placing a small sample from the non magnetic fraction under a binocular (using white light) and checking that no dark or opaque mineral grains are visible and that the extracted fraction is essentially quartz. Further tests for the presence of feldspar are routinely carried out during OSL measurements using the presence and magnitude of the IRSL signal. In 95% of the samples prepared at the GSI laboratory the IRSL signal is less than 5% of the total OSL signal (measured as the ratio between an ordinary recycling point and an additional post IR recycling point).

For fine sand sediment (74 to 180 µm) the optimal setting was found to be:

Slope of 25°, tilt of 17°
Current -1.4-1.5 Amp on the magnet
Sample flow rate: 2-3 g/min

One run through the magnetic separator is usually sufficient to extract clean quartz. Re-running the magnetic fraction may result in extracting a few additional quartz grains and this is recommended when sample size is very small. Re-running the non magnetic quartz fraction is not necessary as this fraction will undergo etching with HF.

The magnetic fraction in a sample may vary between 10 and 70% of the sample. In some cases the magnetic fraction contains quartz grains which will not be separated by a second pass through the magnet. Usually those are quartz grains coated by iron oxides or containing heavy mineral inclusions. Reducing the current on the magnet to 1.2-1.3 Amp may increase the yield of this type of quartz into the non-magnetic fraction.

For most samples the great majority of feldspar grains are removed by magnetic separation. As it is then not necessary to dissolve large quantities of feldspars, only small amounts of HF are needed for obtaining pure quartz. Stoichiometrically, only 2 cm^3 of concentrated (40%) HF per 1 g of quartz are necessary for dissolving the quartz, however routinely much more is used when dissolving feldspar. We found experimentally (by checking for the presence of IR signals as mentioned above) that for the majority of samples, 5 cm^3 HF per 1 g quartz

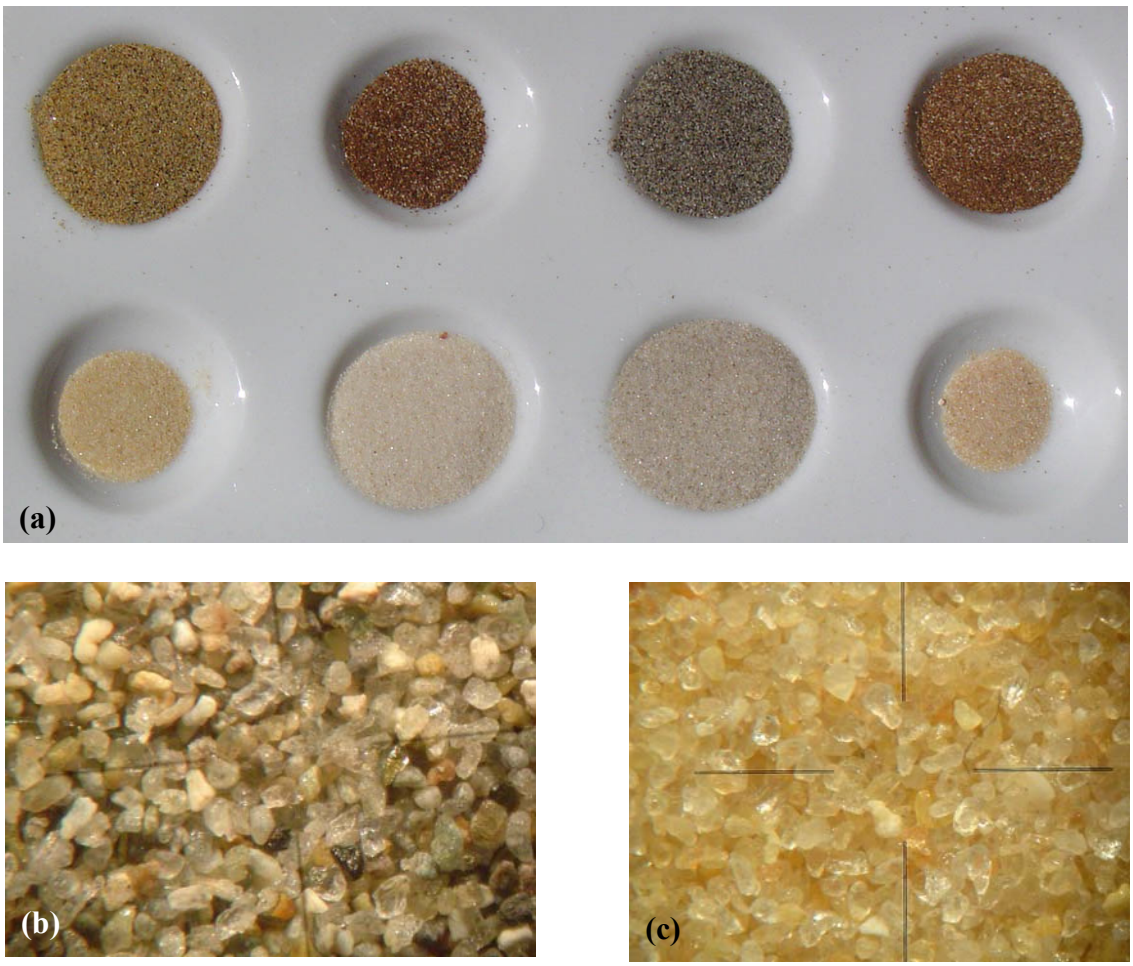

Figure 2: *Images of samples after magnetic separation. The non magnetic fraction is essentially pure quartz.*
(a) Magnetic (top) and non magnetic (bottom) fraction of four sand samples.
(b) Close up of sample before magnetic separation. Note abundant quartz, feldspar (pale, opaque) and some heavy mineral grains (125-150 µm).
(c) Close up of the non-magnetic fraction. A few remaining feldspar grains are visible (125-150 µm).

will remove any remaining feldspars while etching the quartz. A smaller volume of HF occasionally resulted in IR signals. It should be noted that even in samples with some IR signal, the amount of feldspar remaining after HF etching is so low that it cannot be detected with X-ray diffraction.

Practicalities

The model used in this study is the Frantz Magnetic Barrier Laboratory Separator Model LB-1, which is about 15 years old (for more information see http://www.sgfrantz.com/labsep.htm). The separator is located in a light-tight room and can be used either under normal neon lights or with subdued orange lights. It is shared with other geologists requiring mineral separation. Using it is very straight forward and students can use it independently after a single demonstration.

A binocular microscope in the laboratory is necessary, used to examine tiny amounts of the magnetic and non magnetic fractions under white light, to verify that separation was successful and that essentially only quartz is present in the non-magnetic fraction. Cleaning between samples is carried out using pressurized air and a brush.

Magnetic separators are usually found in geology and mineralogy departments. The most common instruments are made by S.G. Frantz Company, Inc. Before making any major purchases, it is worth going to the nearest laboratory with a magnetic separator to try out a sample that can be exposed to light. The

features one should look for are ease of operation in semi darkness and the stability of the magnetic field. In very old models the magnet tends to overheat and the current on the magnet drifts to lower values.

In most dating labs, magnetic separators will be used only for part of the time. Since the cost of a modern magnetic separator is in the range of US$18,000, it is worth considering buying it jointly (or using an available one) with other departments. As long as the laboratory can be made light-tight and fitted with appropriate lighting for OSL sample preparation, sharing an instrument is feasible.

References

Aitken, M.J. (1985) *Thermoluminescence Dating*. Academic Press, London.

Augusto, P.A., and Martins, J.P. (1999) A new magnetic separator and classifier: Prototype design. *Minerals Engineering* **12**, 799-807.

Fleming, S.J. (1966) Study of thermoluminescence of crystalline extracts from pottery. *Archaeometry* **9**, 170-173.

Kolodner, K., Avigad, D., McWilliams, M., Wooden, J. L., Weissbrod, T., and Feinstein, S. (2006) Provenance of north Gondwana Cambrian–Ordovician sandstone: U–Pb SHRIMP dating of detrital zircons from Israel and Jordan. *Geological Magazine* **143**, 367–391.

Rosenblum, S. (1958) Magnetic susceptibilities of minerals in the Franz isodynamic magnetic separator. *American Mineralogist* **47**, 170-173.

Wintle, A. G. (1997) Luminescence dating: laboratory procedures and protocols. *Radiation Measurements* **27**, 769-817.

Reviewer

Andrew Murray

A Linear Modulation OSL Study of the Unstable Ultrafast Component in Samples from Glacial Lake Hitchcock, Massachusetts, USA

R.J. Goble[1] and T.M. Rittenour[1,2]

1. Department of Geosciences, University of Nebraska-Lincoln, 214 Bessey Hall, Lincoln, Nebraska, USA 68588-0340 (e-mail: rgoble2@unl.edu)
2. Current Address: Department of Geology, Utah State University, 4505 Old Main Hill, Logan, Utah, USA 84322

(Received 20 April 2006; in final form 14 November 2006)

Abstract
Optical ages were determined for samples from delta and sand dune deposits associated with Glacial Lake Hitchcock near Amherst, Massachusetts using the single aliquot regenerative-dose (SAR) optically stimulated luminescence (OSL) technique. However, a strong unstable ultrafast component caused initial rejection of data from a large proportion of aliquots. A linearly modulated blue OSL (LM-OSL) study was undertaken on the sample with the strongest ultrafast component, with the data modelled using the equation of Bulur et al. (2000) as 5 fast, medium and slow components, and 1 ultrafast component.

The ultrafast component dominates the LM–OSL, almost completely obscuring the fast component. As suggested by Jain et al. (2003), the thermal stability of the ultrafast component was examined, using temperatures between 180°C and 300°C (10s preheat) and extended preheats at 300°C (10-60s). Preheats of sufficient stringency to remove the ultrafast component (300ºC for ≥ 20s) also strongly depleted the fast component. The stabilities of the ultrafast and fast components were also examined as a function of low-power, short-duration continuous-wave blue-light stimulations (CW-OSL). A 3.0s, 0.35 mW.cm^{-2} (1% diode power), 125ºC preshine in combination with a 240ºC/10s preheat removed the ultrafast component, and caused significantly less fast component depletion than more stringent preheats. Data from a modified SAR procedure in which each OSL measurement is preceded by a low-power preshine have improved recycling ratios and reduced equivalent dose (D_e) errors. D_e values and resultant ages determined using the preshine-based SAR proposed here are consistent with regional age constraints on the delta and sand dune samples from Glacial Lake Hitchcock.

Keywords
Ultrafast OSL component, Linear Modulation OSL, Glacial Lake Hitchcock

Introduction
Samples of eolian and deltaic sand associated with Glacial Lake Hitchcock near Amherst, Massachusetts (Rittenour, 1999; Rittenour and Brigham-Grette, 2000; Rittenour et al. 2000) were analyzed using the single aliquot regenerative (SAR) protocol (Murray and Wintle, 2000), using sample preparations as outlined in Rittenour et al. (2003, 2005). Analysis was carried out on a Risø TL/OSL-DA-15B/C reader with blue-green (470±30 nm; maximum power 35 mW.cm^{-2}) and infrared LEDs and a 7.5-mm Hoya U340 filter (340±50 nm) (Bøtter-Jensen et al., 2000). The software version of the MiniSys code was 1.11. In screening SAR optically stimulated luminescence (OSL) data using rejection criteria, consistent problems were noted with recycling ratios and equivalent dose (D_e) errors calculated from growth curves, resulting in an unusually large scatter in equivalent dose (D_e) values and a high proportion of data discarded. The problems were traced to the presence of a strong unstable ultrafast component (Jain et al. 2003, Choi et al. 2003). A linearly modulated OSL (LM-OSL) study was undertaken on the sample showing the strongest ultrafast component (GLH-06-09-782, Table 5) to determine a method for removing this component. LM-OSL studies were carried out by ramping the stimulation light intensity from 0 to 35 mW.cm^{-2} (100% power) over 3000s (3000 channels), following a 250Gy irradiation. All LM-OSL measurements were carried out at 125°C on a single aliquot of the sample GLH-06-09-782. Because of the low sensitivity of this and other Glacial Lake Hitchcock samples, large (5 mm) aliquots of 90-125, 90-150 or 150-180 μm quartz sand were used in all OSL analyses.

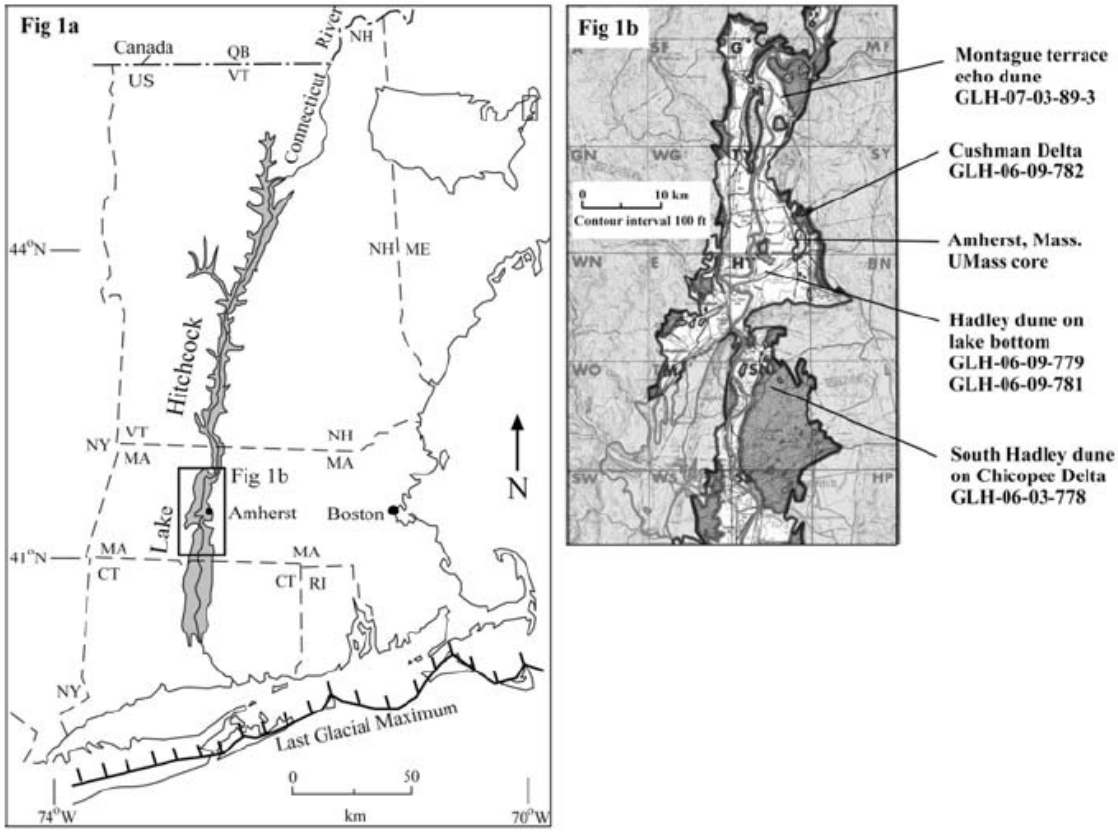

Figure 1: *Location of Glacial Lake Hitchcock within the Connecticut River valley in the northeastern United States.*

Study area

Samples for OSL dating were collected from relic delta and sand dune deposits from Glacial Lake Hitchcock, near Amherst in central Massachusetts (Figure 1). Glacial Lake Hitchcock formed in the Connecticut River valley during retreat of the Laurentide ice sheet at the close of the last glaciation. As the ice margin retreated northward, the lake formed behind a sediment dam in central Connecticut and extended 320 km to the north within the Connecticut River valley into northern Vermont. A count of annual varves from the lake basin indicates that the lake existed for over 4000 years (Antevs, 1922; Ridge et al., 1999, 2001; Rittenour, 1999). Radiocarbon age control from the New England (NE) varve chronology suggests that Glacial Lake Hitchcock formed prior to 15.0 ^{14}C kyr BP and drained by 11.8 ^{14}C kyr BP (~18.0 and ~14.0 cal kyr BP) (Ridge et al., 1999), although recent re-correlations suggest the lower portion of the NE varve chronology may be 700 years older (Ridge, 2003). During the existence of the lake, large deltas formed at the mouths of tributaries entering the lake basin. Subsequent to lake drainage, sand dunes formed on the exposed non-vegetated lake bottom, deltas and early terraces cut by the Connecticut River (Rittenour, 1999; Rittenour and Brigham-Grette, 2000). OSL samples were collected from these pre-drainage delta deposits and post-drainage eolian deposits in order to better constrain the timing of lake drainage.

Modelling of LM-OSL data

A background correction was determined by averaging the LM-OSL (3000 channels, 3000 seconds, 0 to 35 mW.cm^{-2} (100%) diode power, 125ºC) on two blank aluminium disks coated with Silkospray^{TM}. The LM-OSL background (Figure 2) shows an increase in intensity with applied power, similar to the background observed in the LM-OSL study of Choi et al. (2006); the data were fitted with a third order polynomial. A similar background, with somewhat lower intensities at higher powers was observed using a stainless steel disk during LM-OSL measurements; this finding was also checked by setting the diode power to various levels (0, 10, 20, 30…90, 100%) and measuring the background signal. These continuous wave OSL (CW-OSL) data are also shown on Figure 2, and show a similar pattern of increase. A similar CW-OSL measurement of the background using infrared diodes (125ºC) does not show the increase in intensity with power. The

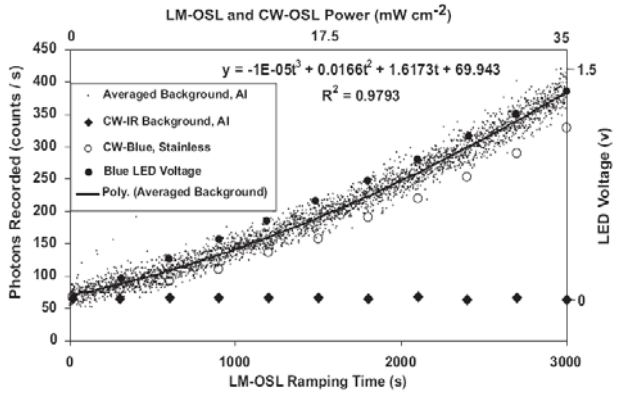

Figure 2: *LM-OSL and CW-OSL data, collected while holding the sample at 125°C, from a sample disk coated with SilkosprayTM, following 250 Gy irradiations and 240ºC/10s preheats. LM-OSL data represent the average of two measurements; CW-OSL measurements are averaged photon counts per second (100s acquisition) at the specified power (upper scale). An aluminium disk was used, unless otherwise noted in the legend. Blue LED voltages measured at the test point on the rear of the Minisys are also shown, referenced to the right-hand scale.*

voltage applied to the blue LEDs as a function of applied power is also shown in Figure 2. These data show no curvature within the error of the measurement (0.01 volts), and we conclude that the non-linearity in the background is due to increased filter breakthrough with increased power to the diodes, rather than non-linearity in the intensity of the light emitted by the LEDs. In a similar LM-OSL study, Choi et al. (2006) demonstrated that the increase in intensity of light emitted by their diodes was linear, although the background count rates from a blank disk were non-linear, and attributed the non-linearity to possible slight changes in wavelength of the LED emission with power increase, allowing more photons to pass through the filter. A background blue LM-OSL correction based on the calculated polynomial has been applied to all subsequent data sets prior to peak fitting.

LM-OSL measurements (0 – 35 mW.cm^{-2}, 3000 s, 3000 channels) were conducted on the natural GLH-06-09-782 sample and the same aliquot following a 250 Gy irradiation (Figure 3). A 240ºC/10s preheat and 125ºC measurement temperature were used. The natural signal has been multiplied by 10 for comparison purposes. The irradiated sample has a strong ultrafast component, which dwarfs the other peaks; this peak is not present in the natural sample and is thus assumed to be unstable over the age of this sample. This unstable ultrafast component is similar to that noted by Jain et al. (2003).

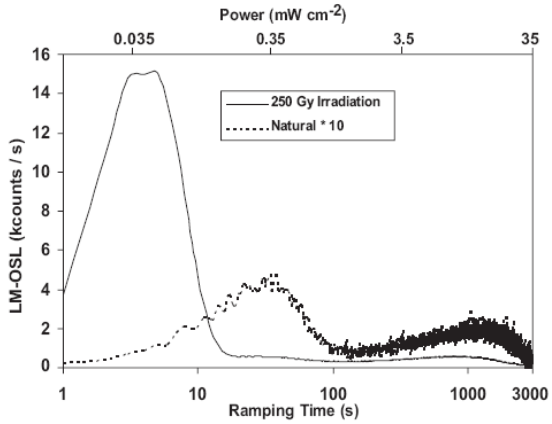

Figure 3: *Natural LM-OSL (multiplied by 10) and LM-OSL following a 250 Gy irradiation (240ºC/10s preheat, 125ºC measurement).*

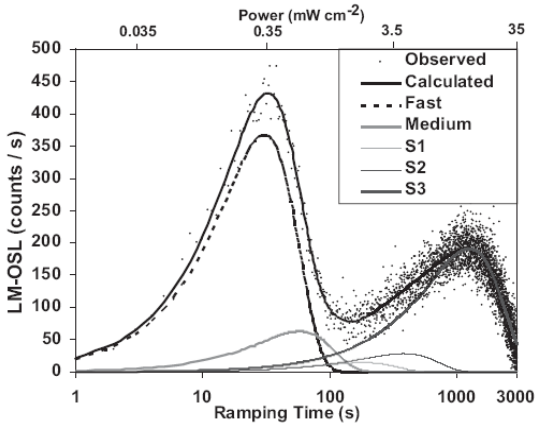

Figure 4: *Natural LM-OSL, fitted with five components using the equation of Bulur et al. (2000). Component designation follows Singarayer et al. (2003).*

The natural LM-OSL data (Figure 4) can be adequately modelled as the sum of five peaks, using the equation of Bulur et al. (2000). As shown in Table 1, relative values of σ (Choi et al., 2006) for these components are similar to those observed by Singarayer and Bailey (2003), and their notation has been followed in this study. These five peaks plus an ultrafast peak, where present, were used in fitting the data from all subsequent experiments.

Change in signal components as a function of preheat temperature

Jain et al. (2003) noted that the ultrafast component in their sample could be eliminated by heating to 260ºC; Choi et al. (2003) obtained satisfactory results using a test dose cut-heat of 220ºC. LM-OSL runs were conducted on GLH-06-09-782 between 180ºC/10s and 300ºC/10s, at 20ºC intervals, in order to determine the preheat temperature necessary for elimination of the ultrafast component (Figure 5a,

Jain et al. (2003)		Singarayer and Bailey (2003)		This Study	
Component	Relative σ	Component	Relative σ	Component	Relative σ
Ultrafast	13	Ultrafast	28	Ultrafast	27
Fast	1	Fast	1	Fast	1
Medium	0.2	Medium	0.2	Medium	0.1
Slow 1	0.06				
Slow 2	0.01	S_1	0.01	S_1	0.01
Slow 3	0.001	S_2	0.001	S_2	0.001
Slow 4	0.0001	S_3	0.0001	S_3	0.0003

Table 1: *Comparison of relative values of σ and the notation used by Jain et al. (2003), Singarayer and Bailey (2003), and this study.*

5b). The 300ºC preheat was repeated at 10 second intervals between 10 and 60s. Signal change is measured relative to the photon sum rather than the maximum photon count. Sensitivity change in the ultrafast and fast components, as monitored with a small test dose, is shown in the upper part of Figure 5b; corrections have been applied to the data in the lower part of Figure 5b (the apparent sensitivity change shown by comparing 240ºC peak intensities in Figures 3 and 5 is probably related to a changed electronic board in the Minisys). As noted by Packman et al. (in press), the ultrafast and fast components sensitize differently, particularly at temperatures above 240ºC. The ultrafast component (Figure 5b) is still present at 260ºC, but has been almost entirely removed by a 300ºC/10s preheat, although the 300ºC preheat must be maintained for at least 20 seconds (Figure 5a) to fully remove the ultrafast component. Other signal components show similar depletions with increased stringency of preheat. Increasing the preheat from 240ºC to 300ºC/20s depletes the fast component from 64±5% of the initial 180ºC intensity to 36±3%. The additional 56±6% depletion below the signal level remaining after a 240ºC preheat could be problematic in this low-response sample. Therefore, an alternate approach to removal of the ultrafast component was sought.

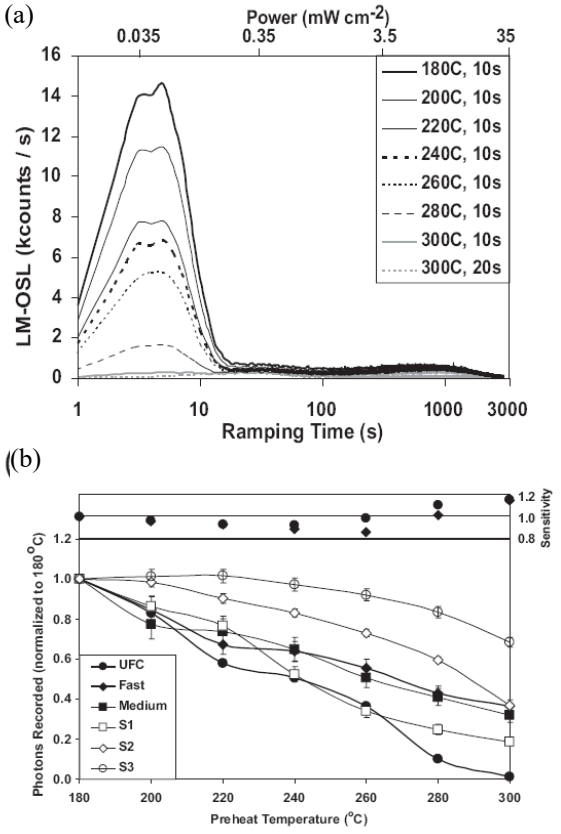

Figure 5: *a) LM-OSL following preheats at various temperatures and times (250 Gy applied dose, 125ºC measurement). b) Changes in signal strength for the six components required to model the LM-OSL signal. Changes in sensitivity for the ultrafast and fast components are shown in the upper part of the figure.*

Depletion of signal components as a function of CW-OSL power

Use of a low-power bleach to remove the ultrafast component was explored as an alternative to a more stringent preheat. The sample was given a 250 Gy dose, followed by a 240ºC/10s preheat and a 10 s CW-OSL at diode powers between 0 to 0.35 mW. cm^{-2} (1%), followed by a 3000s, 3000 channel, 0 – 35

mW.cm^{-2} (100%) diode power LM-OSL measurement at 125ºC. There was no measurable change in the LM-OSL curves below 0.5% CW-OSL power setting, or between 0.5% and 1% CW-OSL power, suggesting that the system software interprets CW-OSL values below 0.5% as 0% power and values between 0.5% and 1% as 1% power, an observation confirmed by Duller (pers. comm., 2006). With ≥ 0.35 mW.cm^{-2} (1% diode power), the ultrafast component was completely removed, and the fast component was depleted by 24±2%. This compares favourably with the 64±3% depletion associated with a preheat of sufficient stringency (300ºC/20s) to remove the ultrafast component, even allowing for the different effect of a 180ºC/10s vs 240ºC/10s preheat in these experiments. A 0.35 mW.cm^{-2} (1%) power-level setting was used for all subsequent low-power bleaching experiments. The lack of change in the LM-OSL curves through five cycles of 0% CW-OSL preshines or six cycles of 1% CW-OSL preshines also demonstrates that the long LM-OSL measurements are sufficient to remove the signal prior to the next cycle of measurements.

Depletion of signal components with CW-OSL time at 0.35 mW.cm^{-2} (1%) power

The time needed for a 1% CW-OSL preshine to remove the ultrafast component was explored by applying a 250 Gy dose, followed by a 240ºC/10s preheat and a short CW-OSL 0.35 mW.cm^{-2} (1%) power "preshine" at times from 0 to 3 seconds, followed by a 3000s, 3000 channel, 0 – 35 mW.cm^{-2} (100%) power LM-OSL at 125ºC to measure remaining peak intensities; sensitivity corrections, as determined from a small test-dose following the LM-OSL, were applied to the ultrafast and fast components. LM-OSL curves with and without a 3 second preshine are shown in Figure 6a. Changes in intensity for all components, in 0.25s time-increments, are shown in Figure 6b. Sensitivity changes in the ultrafast and fast components are shown in the upper part of Figure 6b; there is < 1% difference between the values. Decay curve data collected for the 3.0 s CW-OSL preshine are also shown. A 2.5 to 3.0 s 0.35 mW.cm^{-2} (1%) power preshine is sufficient to reduce the ultrafast component to a level similar to that observed using a 300ºC/20s preheat (~99% removed). The fast component is depleted by approximately 8±4% at 3.0s. This compares favourably with the 56±6% depletion in the fast component produced by increasing the preheat from 240ºC/10s to 300ºC/20s in order to fully remove the ultrafast component.

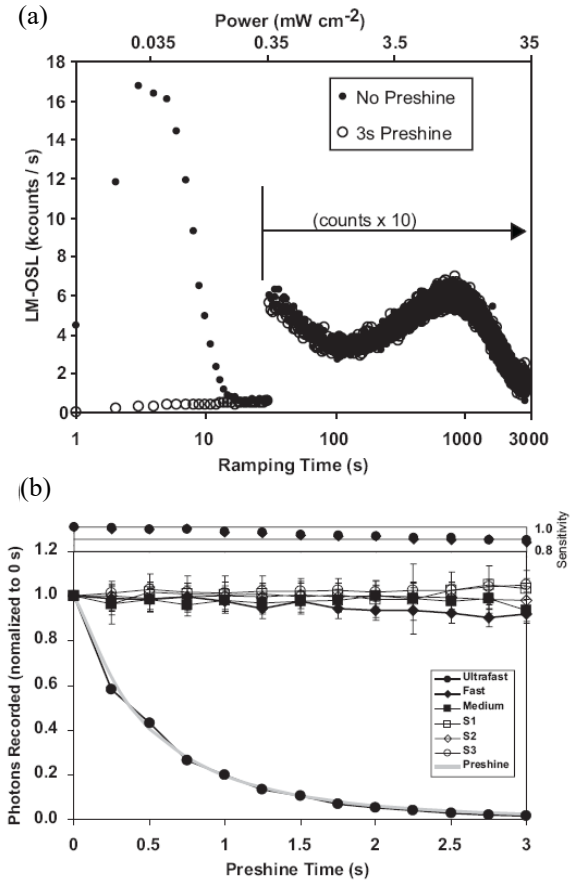

Figure 6: *a) LM-OSL with and without a 3 s, 0.35 mW cm-2 preshine (250Gy applied dose, 240ºC/10s preheat, 125ºC measurement); counts at ramping times greater than 30 s have been multiplied by 10. b) Relative change in intensity of the ultrafast and fast components as a function of CW-OSL 0.35 mW cm-2 (1%) diode power preshine times. Changes in sensitivity for the ultrafast and fast components are shown in the upper part of the figure.*

Sensitivity changes as a function of cutheat/ preheat temperature

Packman et al. (in press) have shown that sensitivity change in a sample with an ultrafast component is a function of preheat/cutheat temperature, requiring the use of the same temperature (200ºC for their samples) for both preheat and cutheat in applying the SAR procedure. This is also shown by the sensitivity data in Figure 5b. Sensitivity changes as a function of variations in cutheat and preheat temperature in sample GLH-06-09-782 were monitored by running the sequence shown in Table 2. The sensitivity change in the preshine data varies with stringency of the cutheat/preheat (Figure 7a). However, the decay-curve data measured subsequent to the preshine show

	Operation
1	200s beta (~20 Gy)
2	160°C/0s cutheat
3	2s preshine (1% power, 125ºC)
4	40s OSL (90% power, 125ºC)
5	200s beta (~20 Gy)
6	220°C/0s cutheat
7	2s preshine (1% power, 125ºC)
8	40s OSL (90% power, 125ºC)
9	200s beta (~20 Gy)
10	240°C/10s preheat
11	2s preshine (1% power, 125ºC)
12	40s OSL (90% power, 125ºC)
13	200s beta (~20 Gy)
14	260°C/10s preheat
15	2s preshine (1% power, 125ºC)
16	40s OSL (90% power, 125ºC)
	Repeat cycle (1) to (16) 3 times

Table 2: *Sequence used to determine sensitivity change with cutheat and preheat temperature. 1% power corresponds to 0.35 mW.cm^{-2}.*

	Operation
1	Apply dose (0 for natural)
2	Preheat, 260°C/10s
3	3.0s preshine CW-OSL (1% power, 125°C, 10s pause)
4	40s CW-OSL (90% power, 125°C, 10s pause)
5	Test dose irradiation
6	Cutheat, 220°C/0s
7	3.0s preshine CW-OSL (1% power, 125°C, 10s pause)
8	40s CW-OSL (90% power, 125°C, 10s pause)
9	Repeat (1) through (8) for regenerative doses
10	Calculate L_x/T_x from (4) and (8)

Table 3: *Modified SAR sequence used to remove ultrafast component. 1% power corresponds to 0.35 mW.cm^{-2}.*

little, if any, dependence on stringency of cutheat/preheat, making it unnecessary to use the same cutheat/preheat conditions if a preshine is used. The ultrafast component is most dominant in the lower temperature preheat/cutheat preshine decay curves (Figure 7b), as would be expected from the data in Figure 5 and the study by Jain et al. (2003). Therefore, unless removed by a preshine, an unstable ultrafast component will more strongly affect test-dose measurements than regenerative-dose

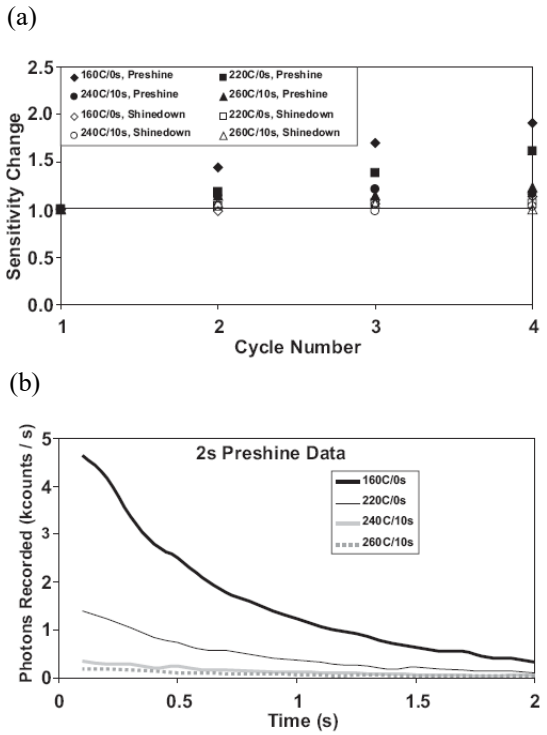

Figure 7: *a) Sensitivity change as a function of cutheat and preheat temperature and cycle number. b) Preshine data (0.35 mW.cm^{-2} power) for the fourth cutheat and preheat cycle shown in Table 2.*

measurements, because generally a less stringent cutheat is used as opposed to preheat (Murray and Wintle, 2000). Jain et al. (2003) show that different OSL components do not always sensitize in the same manner.

Application to OSL samples, glacial Lake Hitchcock

Table 4 compares results for sample GLH-06-09-782 for the conventional SAR procedure with results for the modified SAR with preshine procedure (Table 3); data are included for all aliquots (0 rejected, criteria = none), and for aliquots rejected if recycling or D_e errors exceed 10% (criteria = 10%, data in boldface type). The average percent absolute error on the recycling ratio and average percent error on the equivalent dose are tabulated in Table 4; other rejection criteria were also monitored (test dose error, decay curve characteristics, feldspar contamination, D_e > regenerative doses), but have not been tabulated.

The conventional SAR procedure (Method: SAR) resulted in a large error on both tabulated criteria, and a large proportion of rejected aliquots (17 of 19 rejected). The preshine-SAR procedure (Method: ps-SAR) reduced the errors on these rejection criteria, and resulted in a smaller proportion of rejected aliquots (6 of 25 rejected). Finally, the conventional

Method	Rejected Aliquots (Criteria)[a]	Average Recycling Ratio, (%)[b]	Average D_e Error (%)[c]	D_e (± 1σ)[d]
SAR	0 of 19 (none)	0.87 (19%)	15.22	34.44 ± 3.60
SAR	**17 of 19 (10%)**	**0.98 (3%)**	**6.10**	**21.86 ± 2.92**
ps-SAR	0 of 25 (none)	0.96 (8%)	5.04	32.76 ± 2.83
ps-SAR	**6 of 25 (10%)**	**0.97 (5%)**	**4.35**	**29.83 ± 1.10**
ps-SAR (150-180µm)	**14 of 40 (10%)**	**1.01 (5%)**	**4.76**	**29.77 ± 1.22**
SAR, omit channel 1	0 of19 (none)	1.05 (13%)	22.93	23.13 ± 1.97
SAR, omit channel 1	**15 of 19 (10%)**	**1.05 (6%)**	**3.18**	**29.53 ± 4.38**

Notes:
a: Rejection criteria (none = no aliquots rejected, 10% = aliquots with recycling ratio and De error >10%); other rejection criteria were also monitored
b: Average percent absolute error on the recycling ratio
c: Average percent error on the equivalent dose
d: 1 standard error
90-125 or 90-150µm grains, unless otherwise noted

Table 4: *OSL data for the Cushman Delta (GLH-06-09-782) sample. Data selected/rejected using normal (i.e. 10%) rejection criteria are in boldface type. Methods used are discussed in the text.*

Sample #	Lab #	Method	Aliquots[a]	Dose Rate	D_e (± 1σ)[b]	Age (ka)
DELTAIC DEPOSITS, 14-18 ka[c]:						
Cushman Delta (strong ultrafast)						
GLH-06-09-782	UNL-558	SAR	2 of 19	2.02 ± 0.05	21.86 ± 2.92	10.8 ± 1.5
GLH-06-09-782	UNL-558	ps-SAR	19 of 25	2.02 ± 0.05	29.83 ± 1.10	14.8 ± 0.8
GLH-06-09-782	UNL-558	ps-SAR (150-180µm)	26 of 40	2.02 ± 0.05	29.77 ± 1.22	14.7 ± 0.8
DUNE DEPOSITS, < 14 ka[c]						
Hadley dune on lake bottom (weak ultrafast)						
GLH-06-09-779	UNL-556	SAR	11	1.47 ± 0.05	17.80 ± 1.49	12.1 ± 1.1
GLH-06-09-779	UNL-556	ps-SAR	21	1.47 ± 0.05	16.97 ± 0.81	11.6 ± 0.7
GLH-06-09-781	UNL-557	ps-SAR	19	1.81 ± 0.06	19.51 ± 1.09	10.8 ± 0.8
Montague echo dune on early terrace cut into Montague delta (weak ultrafast)						
GLH-07-03-89-3	UNL-554	ps-SAR	21	1.37 ± 0.04	18.16 ± 0.73	13.3 ± 0.8
South Hadley dune on Chicopee delta						
GLH-06-03-778	UNL-555	ps-SAR	28	2.08 ± 0.06	25.74 ± 1.46	12.4 ± 0.9

Notes:
a: Aliquot rejection based on D_e error, recycling ratio, test dose error, decay curve characteristics, feldspar contamination, D_e > regenerative doses
b: 1 standard error
c: Age constraints from varve and radiocarbon chronology
ps-SAR: SAR following a 3s 1 % power CW-OSL preshine
grain size is 90-125 or 90-150µm, unless otherwise noted

Table 5: *Comparison of optical ages of samples from Glacial Lake Hitchcock determined using SAR and ps-SAR with a 1% diode power (0.35 mW cm^{-2}) 3 s preshine.*

SAR data were recalculated but channel 1 (0.17s; total power 31.5 mW.cm^{-2}), which should contain the ultrafast component, was omitted (Method: SAR, omit channel 1). This produced a data set with large errors on the D_e values and a large number of rejected aliquots (15 of 19 rejected). The large number of rejected aliquots is believed to be due to removal of not only the ultrafast component, but also a large proportion of the fast component from this low response sample. The D_e values determined using normal rejection criteria and the preshine-SAR (both 90-150 and 150-180μm), and conventional SAR omitting channel 1 are almost identical, and differ significantly from the conventional SAR (channel 1 included) of the data (Table 4). However, the preshine-SAR is the only technique which did not result in a large number of rejected aliquots.

Samples from Glacial Lake Hitchcock were re-analyzed using the modified SAR with preshine sequence (Table 3). Results are shown in Table 5. SAR dose rates were determined as outlined in Rittenour et al. (2003, 2005) using the cosmic dose rate equations of Prescott and Hutton (1994) and the dose rate conversion factors of Adamiec and Aitken (1998). Errors were calculated in quadrature using the methods of Aitken and Alldred (1972) and Aitken (1976, 1985). Only sample GLH-06-09-782 showed the presence of a strong ultrafast component, although a weak ultrafast component was detected in three other samples. Using the SAR technique with a 0.35 mW.cm^{-2} (1%) 3s preshine increased the determined age for sample GLH-06-09-782 by 4 ka, beyond the combined 1-sigma error bars.

The ultrafast component in GLH-06-09-782 showed grain-size dependency, and was not detected in LM-OSL studies of the coarser 150-180 and 180-212μm fractions, although subsequent preshine-SAR analyses showed it to be present as a minor component. The coarser fraction was analyzed using the preshine-SAR method, with results which are consistent with preshine-SAR data from the 90-150μm fraction (ps-SAR, Table 5). The SAR with preshine ages for all samples are consistent with varve and radiocarbon age constraints from the lake basin (see below).

Comparison of OSL ages to other age constraints

Samples for OSL dating were collected from a high-stand delta of Glacial Lake Hitchcock and several post-drainage sand dunes from the lake bottom, an early terrace and an abandoned delta surface. These samples were carefully selected to bracket the timing of lake drainage within central Massachusetts.

In addition to the fairly well-dated NE varve chronology (Ridge et al., 1999, 2001), the timing of ice retreat, duration of lake existence, and the timing of lake drainage in central Massachusetts are constrained by a varve-sequence core collected from the University of Massachusetts-Amherst campus (UMass core, Figure 1b) (Rittenour, 1999; Rittenour et al., 1999; Rittenour and Brigham-Grette, 2000). The UMass core extends to 32m depth below the lake bottom surface and covers a sequence of 1,389 varves that transition from thick pro-glacial varves immediately above bedrock to thin distal varves at the top of the sequence. A radiocarbon age obtained from a sample collected near the top of the core (NE varves 5761-5768, 12,370 ± 120 ^{14}C yr BP, Beta 124780; ~14.5 ± 0.5 cal ka using INTCAL04, Reimer et al., 2004) indicates that the UMass core covers the interval from 15.6 – 14.2 ± 0.5 cal ka, consistent with the chronology of Ridge et al. (1999). Based on this core and the NE varve chronology, the ice margin retreated north of Amherst MA by 15.6 ± 0.5 cal ka (first varve deposited over bedrock) and Glacial Lake Hitchcock drained in this region sometime after 14.2 ± 0.5 cal ka (last varve deposited in core) (Rittenour, 1999), providing a narrower time frame for the duration of lake existence in central Massachusetts than the entire length of the varve chronology (4000 years).

Assuming the UMass core chronology and the NE varve chronology are correct, deltas into Glacial Lake Hitchcock could only have formed after ice retreat from the region but before lake drainage (15.6-14.2 ± 0.5 cal ka), and sand dunes on the lake bottom, early terraces and abandoned deltas could only have formed after the lake drained (after 14.2 ± 0.5 cal ka). The OSL ages obtained from the preshine-SAR method are consistent with these age constraints and indicate that topset beds from the Cushman Delta (GLH-06-09-782) are 14.7-14.8 ± 0.8 ka and sand dunes in the region formed between 13.3 ± 0.8 cal ka and 10.8 ± 0.8 ka (Table 5).

Conclusions

The following conclusions can be made with respect to the LM-OSL study of samples from Glacial Lake Hitchcock:

1. Blue LM-OSL background is a rising curve modelled with a third-order polynomial. Voltage applied to the stimulating LEDs is linear, within the error of the measurements.

2. A strong ultrafast component present in sample GLH-06-09-782 from Glacial Lake Hitchcock was preferentially removed using a 0.35 mW. cm^{-2} (1%) power 3s CW-OSL sequence prior to

each OSL measurement in the SAR protocol. This produced a reduction in the ultrafast component similar to a stringent 300°C/20s preheat, but with much less relative reduction in the fast component.

3. Differential sensitivity changes in the preshine data are observed as a function of stringency of cutheat and preheat. This results in inappropriate sensitivity corrections in the conventional SAR procedure, since prior heating is different for regenerative and test doses. This is reflected in problems with the recycling ratio and equivalent dose errors, and results in a large number of rejected D_e determinations based upon these criteria. If a preshine is not used to remove the ultrafast, the cutheat and preheat conditions must be the same, as noted by Packman et al. (in press). However, that will still lead to erroneous D_e values because of the presence of the thermally unstable ultrafast component in regenerative OSL data but its absence in the natural OSL data (Jain et al. 2003).

4. The improvement in errors in calculated D_e and recycling ratio criteria using a preshine are due to the correction of the differential sensitivity change between test-dose and regenerative-dose data, whereas changes in the D_e values will also be due in part to removal of the unstable ultrafast from the regenerative dose as opposed to natural data. The use of a preshine drastically reduced the rejection rate for D_e determinations.

5. OSL curves measured subsequent to the preshine show no sensitivity dependency upon cutheat/preheat conditions (160°C/0s, 220°C/0s, 240°C/10s, 260°C/10s).

6. Optical ages determined using the SAR procedure with a preshine are compatible with varve and radiocarbon age constraints.

Acknowledgements

We thank Mayank Jain for helpful comments on the early stages of this research and for rigorous and helpful review of the manuscript, and Julie Brigham-Grette for assistance in the field and supervision of the M.S. research from which this project developed. This research was supported in part by a University of Nebraska-Lincoln Maud Hammond Fling Faculty Research Fellowship to R.J. Goble.

References

Adamiec, G. and Aitken, M. (1998) Dose-rate conversion factors: update. *Ancient TL* **16**, 37-50.

Aitken, M.J. (1976) Thermoluminescent age evaluation and assessment of error limits: revised system. *Archaeometry* **18**, 233-238.

Aitken, M.J. (1985) *Thermoluminescence Dating*. Academic Press, London.

Aitken, M.J. and Alldred, J.C. (1972) The assessment of error limits in thermoluminescent dating. *Archaeometry* **14**, 257-267.

Antevs, E. (1922) The recession of the last ice sheet in *New England: American Geographical Society Research Series* **11**.

Bøtter-Jensen, L., Bulur, E., Duller, G.A.T. and Murray, A.S. (2000) Advances in luminescence instrument systems. *Radiation Measurements* **32**, 523-528.

Bulur, E., Bøtter-Jensen L. and Murray, A.S. (2000) Optically stimulated luminescence from quartz measured using the linear modulation technique. *Radiation Measurements* **32**, 407-411.

Choi, J.H., Duller, G.A.T. and Wintle, A.G. (2006) Analysis of quartz LM-OSL curves. *Ancient TL* **24**, 9-20.

Choi, J.H., Murray, A.S., Jain, M., Cheong, C.-S. and Chang, H.W. (2003) Luminescence dating of well-sorted marine terrace sediments on the southeastern coast of Korea. *Quaternary Science Reviews* **22**, 407-421.

Jain, M., Murray, A.S. and Bøtter-Jensen, L. (2003) Characterisation of blue-light stimulated luminescence components in different quartz samples: implications for dose measurement. *Radiation Measurements* **37**, 441-449.

Murray, A.S. and Wintle, A.G. (2000) Luminescence dating of quartz using an improved single-aliquot regenerative-dose protocol. *Radiation Measurements* **32**, 57-73.

Murray, A.S. and Wintle, A.G. (2003) The single aliquot regenerative dose protocol: potential for improvements in reliability. *Radiation Measurements* **37**, 377-381.

Packman, S.C., Mauz, B., Rousseau, D.-D., Antoine, P., Rossignol, J. and Lang, A. (in press) Implications of broad dose distributions obtained with the single-aliquot regenerative-dose method on quartz fine-grains from loess. *Quaternary Geochronology*

Prescott, J.R. and Hutton, J.T. (1994) Cosmic ray contributions to dose rates for luminescence and ESR dating: large depths and long-term time variations. *Radiation Measurements* **23**, 497-500.

Reimer P.J., Baillie, M.G.L., Bard, E., Bayliss, A., Beck, J.W., Bertrand, C., Blackwell, P.G., Buck,

C.E., Burr, G., Cutler, K.B., Damon, P.E., Edwards, R.L., Fairbanks, R.G., Friedrich, M., Guilderson, T.P., Hughen, K.A., Kromer, B., McCormac, F.G., Manning, S., Bronk Ramsey, C., Reimer, R.W., Remmele, S., Southon, J.R., Stuiver, M., Talamo, S., Taylor, F.W., van der Plicht, J. and Weyhenmeyer C.E. (2004) IntCal04 terrestrial radiocarbon age calibration, 0-26 cal kyr BP. *Radiocarbon* **46**, 1029-1058.

Ridge, J.C. (2003) The last deglaciation of the northeastern United States: A combined varve, paleomagnetic, and calibrated ^{14}C chronology: In: D.L. Cremeens and J.P. Hart Eds., *Geoarchaeology of Landscapes in the Glaciated Northeast*, New York State Museum Bulletin **397**, 15-45.

Ridge, J.C., Besonen, M.R. Brochu, M. Brown, S.L. Callahan, J.W. Cook, G.J. Nicholson, R.S. and Toll, T.J. (1999) Varve, paleomagnetic, and ^{14}C chronologies for Late Pleistocene events in New Hampshire and Vermont, U.S.A.. *Geographie physique et Quaternaire* **53**, 1-31.

Ridge, J.C., Canwell, B.A., Kelley, M.A. and Kelley, S.Z. (2001) Atmospheric ^{14}C chronology for late Wisconsin deglaciation and sea-level change in eastern New England using varve and paleomagnetic records: In: T.K Weddle and M.J. Retelle Eds., Deglacial History and Relative Sea-level Changes, Northern New England and Adjacent Canada, Special Paper No. 351, Geological Society of America, Boulder, CO, p. 173-191.

Rittenour, T.M. (1999) *Drainage History of Glacial Lake Hitchcock, Northeastern United States*, Unpublished Masters Thesis, Department of Geosciences, University of Massachusetts, Amherst, 179 p.

Rittenour, T.M. and Brigham-Grette, J. (2000) A Drainage History for Glacial Lake Hitchcock: Varves, Landforms, and Stratigraphy: In: J. Brigham-Grette Ed. North Eastern Friends of the Pleistocene Field Guidebook, Dept of Geosciences Contribution No. 7, University of Massachusetts, Amherst, 125 p.

Rittenour, T.M. Brigham-Grette, J. and Mann, M.E. (2000) El Nino-like climate teleconnections in New England during the Late Pleistocene. *Science* **288**, 1039-1042.

Rittenour, T.M. Goble, R.J. and Blum, M.D. (2003) An optical age chronology of late Pleistocene fluvial deposits in the northern lower Mississippi valley. *Quaternary Science Reviews* **22**, 1105-1110.

Rittenour, T.M. Goble, R.J. and Blum, M.D. (2005) Development of an OSL chronology for Late Pleistocene channel belts in the lower Mississippi valley, USA. *Quaternary Science Reviews* **24**, 2539-2554.

Singarayer, J.S. and Bailey, R.M. (2003) Further investigations of the quartz optically stimulated luminescence components using linear modulation. *Radiation Measurements* **37**, 451-458.

Reviewer

Mayank Jain

The alpha effectiveness in silt-sized quartz: New data obtained by single and multiple aliquot protocols

B. Mauz, S. Packman and A. Lang

Department of Geography, University of Liverpool, Liverpool L69 7ZQ, UK

(Received 29 June 2006; in final form 23 November 2006)

Abstract
The luminescence effectiveness of alpha particles in silt-sized quartz originating from different regions in Europe and North America is presented. Single aliquot regenerative dose (SAR) protocols were used along with the a-value system. The study shows that a-values are independent of a sample's origin, but dependent on the alpha- and beta-doses administered. Sensitivity changes induced by alpha-doses administered during a SAR procedure are not corrected by the beta dose induced test dose OSL. For samples displaying a linear beta-dose response an average a-value of 0.03 was found. For samples exhibiting exponential saturating beta-dose response the a-values determined are higher confirming the dose dependence of the alpha effectiveness in quartz.

Introduction
Quartz is widely used for optical dating. The use of its sand-sized fraction has become the preferred approach in the last few years as this grain size allows the analysis of dose distributions when a small number of grains are used per aliquot and when a single-aliquot regenerative-dose (SAR) protocol is applied. For this grain size, it is assumed that the treatment with hydrofluoric (HF) acid removes the outer rim of the grains which has been affected by alpha radiation in the natural environment. Thus, using sand-sized quartz for optical dating circumvents the need for determining the alpha dose and the alpha dose effectiveness. The silt-sized fraction (4 – 20 μm), however, receives the full alpha dose (α-dose) emitted in the thorium and uranium series and thus, the determination of the alpha dose and its luminescence effectiveness is required.

To determine the alpha effectiveness of a sample, the a-value system (Aitken and Bowman, 1975) is commonly used. Whereas for feldspar silt-sized samples ("polymineral fine grain sample") the a-value has been determined in numerous dating studies (e.g. Lang and Wagner, 1997, Lang et al., 2003), little work has been undertaken to determine the a-value of quartz. Given the relatively low a-values measured for thermoluminescence, typically 0.02 to 0.05 (Aitken, 1985a, p.262), and the mostly insignificant internal radioactivity of natural quartz, there have been few detailed analyses. Rees-Jones (1995) reported a-values of 0.032-0.043 for 4 samples using additive alpha- and beta-dose response curves. Tribolo et al. (2001) for the first time used a SAR protocol to determine the alpha sensitivity of heated quartz. Dating studies (e.g. Stokes et al., 2003a) have used a-values determined on one sample (a = 0.04) and adopted it for the remaining samples or adopted the a-values (e.g. Stokes et al., 2003b) reported by Rees-Jones (1995). It is likely that the luminescence sensitivity of natural quartz for alpha radiation varies little as long as the corresponding alpha- and beta-dose responses are linear. At higher doses, however, less luminescence is created per unit beta-dose; consequently, the contribution of the alpha dose to the total energy deposited increases. The saturation level for beta radiation is grain-dependent (Yoshida et al., 2000), and, thus, the a-value determined using relatively high alpha doses should be sample-dependent and less uniform than the a-value resulting from lower doses.

Our study aimed to test the applicability of a SAR protocol to determine a-values of natural fine-grained quartz particularly with respect to possible sensitivity changes if repeated alpha irradiation is needed. Furthermore, we wished to verify the hypothesis about the dose and sample dependence of the a-value. Silt-sized quartz samples from different areas in Europe and from North America were investigated.

The alpha effectiveness and the a-value system
Alpha particles in the U and Th decay chains have an energy spectrum ranging from 7.8 MeV to zero, where high energy particles travel as far as 47 μm in quartz (Aitken, 1985a, p.253) and affect around 10 mg cm^{-2} (Brennan and Lyons, 1989). The mean absorbed dose fraction for alpha-particles is a function of grain diameter and decreases significantly with grains larger than 20 μm (Bell, 1980). Due to attenuation during travel through matter, the range

spectrum is approximately rectangular, i.e. there is the same number of alpha particles in each interval of range (Aitken, 1985a, p.253). Unlike beta- and gamma-radiation, the luminescence induced by α-radiation is not proportional to energy deposited in a sample but approximately proportional to the total track length deposited and thus, to the travel range of the alpha particle (Brennan and Lyons, 1989). Since the energy deposited per track increases with track length (as the α-particle slows down) the luminescence signal induced in any particular grain by an α-particle is dependent on track length and not just on alpha energy (Brennan et al., 1991). The track length within a grain depends on the diameter of the grain. Thus, the alpha dose absorbed by a silt-sized quartz grain depends on the alpha particle travel range (grain diameter) and energy, whereas the alpha effectiveness depends on track length. The luminescence effects of an α-particle are limited to a small grain volume along the track (Zimmerman, 1972) and consequently, α-particles induce less luminescence for a given amount of absorbed energy than ß-particles and γ-radiation. At higher α-doses tracks overlap and the spatial energy distribution effect of α-particles should disappear (Zimmerman, 1972). Each alpha particle deposits energy only along a small stretch of its track whereas energy deposition by beta particles is not spatially constrained within the crystal. Therefore, at high doses α- and β-growth curves differ (Fig. 1) with the α-growth curve being linear until higher doses than the β-growth curve (Zimmerman, 1972). At doses close to saturation the energy distribution becomes uniform and the luminescence response to α- and β-doses becomes equal (Fig. 1).

Commonly, the a-value system (Aitken and Bowman, 1975) is used to correct the total α-dose rate calculated from the U- and Th-series for the α-effectiveness. The crucial assumptions of the a-value system are:

1. luminescence per unit track length is the same for all alpha particles independent of their energy
2. luminescence per unit of absorbed energy from beta particles is constant and independent of the energy of the particle

The first assumption allows for using a monoenergetic α-source (e.g. ^{241}Am, 3.7 MeV) to monitor the α-effectiveness of a sample in the laboratory. By comparing the beta (or gamma) dose that would induce the same amount of luminescence as the alpha dose from this monoenergetic α-source,

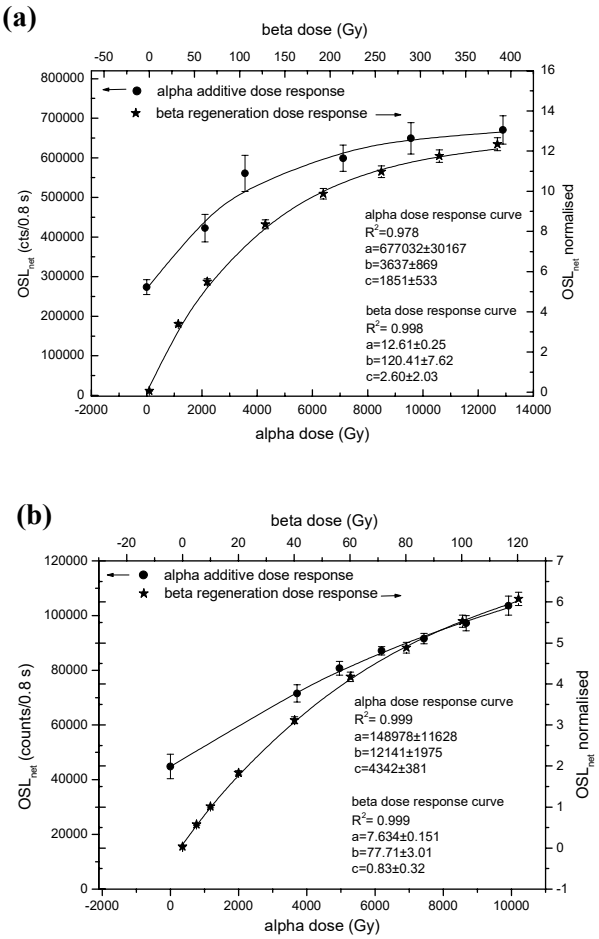

Figure 1: *Alpha- and beta dose response curves of two samples fitted to the equation* $y = a \times (1 - e^{-\frac{x+b}{c}})$. *Each alpha dose point is based on the mean and standard deviation of 3 aliquots after normalisation to the natural OSL. The beta dose points are derived from a SAR measurement of one aliquot. (a) Sample exhibiting a very high natural dose (LV184); (b) sample exhibiting a high natural dose (LV05)*

independence of instrumental and sample sensitivity is achieved. Thus, Aitken (1985a, p.311) gives:

$$\frac{\xi_s v}{\chi_\beta} = 13a$$

where ξ_sv is luminescence per unit alpha track length per unit volume and χß is luminescence per unit absorbed beta dose. The numerical factor is equal to the energy loss per micron for a 3.7 MeV alpha particle in quartz divided by the mass density (Aitken, 1985a). The factor was later considered to be an arbitrary value (Bowman and Huntley, 1984) derived from the transformation from the k-value,

which preceded the a-value system. Bowman and Huntley (1984) show that the ratio

$$\frac{L \cdot per \cdot unit \cdot alpha \cdot track \cdot length}{L \cdot per \cdot unit \cdot absorbed \cdot beta \cdot energy} \text{ (L=luminescence)}$$

accounts for the beta energy that yields the same amount of luminescence as one unit length of alpha track.

Material and experimental details

The samples used here originate from the German North Sea coast (LV03, 04, 05, 06), the South German loess province (LV95, 96, 97), the English east coast (LV17), the English Lake District (LV104) and North America (LV176, 184). Samples were treated in the laboratory following conventional procedures for fine silt (4-20 µm) sample preparation (Mauz et al., 2002) and etched using 20% and 10% hydrofluoric (HF) acid for various durations to remove the feldspar-derived luminescence component (Mauz and Lang, 2004a). After etching the grains, silt from 4-15 µm was separated by settling in acetone. The aliquots of each sample consisted of 2 mg material pipetted onto 1 cm aluminium discs. All samples were tested using infrared stimulation (IR-OSL depletion ratio, Duller, 2003) which examines the effect of the feldspar OSL component on the normalised OSL (L_x/T_x) and thermoluminescence (TL) measurements, which gives an estimate of the amount of feldspars remaining in the sample after chemical treatment (Mauz and Lang, 2004a, Shen et al., in press). According to these tests, all samples used for further experiments were pure quartz samples.

All measurements were performed using an automated Risø TL/OSL reader equipped with an EMI 9635QA photomultiplier and a 40 mCi $^{90}Sr/^{90}Y$ β source, delivering ~0.09 Gy s^{-1} to fine grain quartz on aluminium discs (Mauz and Lang, 2004b). Alpha irradiation was performed in vacuum (10^{-4} mbar), using six 31.6 µCi ^{241}Am sources delivering 3.7 MeV α-particles. The device was built by Bürgi (1992) following the design of Singhvi and Aitken (1978). The sources were calibrated using TLD 200 dosimeters and cross-calibrated with alpha sources at the MPI Heidelberg (Bürgi, 1992). The six sources gave track lengths in the dosimeter between 0.1873 μm^{-2} min^{-1} and 0.2209 μm^{-2} min^{-1}. With respect to the energy deposition in quartz (Aitken, 1985a, p.135 and p.312) these sources delivered doses of 2.44–2.87 Gy min^{-1} on the calibration day (1.3.1991, Bürgi, 1992). These calibration dates were used here as the half life of ^{241}Am is ~ 450 years. Optical stimulation of samples was performed using blue

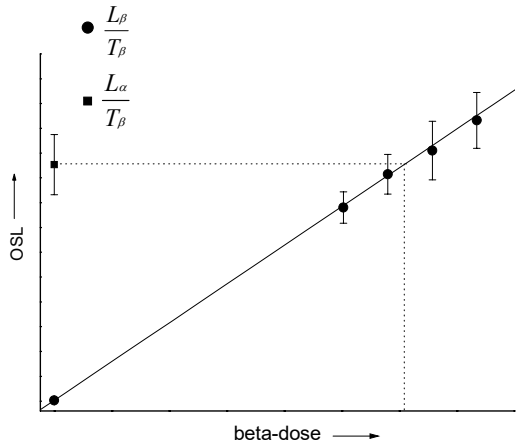

Figure 2: *SAR protocol designed to determine the a-value. The a-value results from the projection of L_α/T_β onto the beta dose response curve obtained from a standard SAR protocol. For details see text.*

LEDs emitting at 470Δ30 nm (delivering ~30 mW cm^{-2}). The OSL was detected through an optical filter (Hoya U340, 7.5 mm) transmitting 260 to 390 nm wavelengths.

To determine the a-value, a SAR protocol was envisaged (Fig. 2). The ß-dose equivalent to a given α-dose should be determined by projecting the regenerated OSL induced by α-irradiation normalised to the OSL of a test dose induced by β-irradiation (L_α/T_β) onto the sensitivity-corrected regenerated dose response curve generated by ß-irradiation. Three experiments were designed to test the reliability of this SAR protocol. In the first experiment the α-dose was given at the end of a standard SAR protocol. The second experiment adopted principles of the dose recovery test (Murray and Wintle, 2003). Aliquots were optically bleached (to remove the natural OSL), given an α-dose, and this was then treated as an unknown dose in the SAR protocol. For this experiment two naturally low-dosed samples (LV04, LV97) were chosen. The third experiment was conducted on aliquots previously used for $D_{eß}$ determination to investigate sensitivity changes. These were subjected to 7 cycles of alpha irradiation (~90 Gy per cycle, sample LV06), preheating and blue light stimulation. Alpha doses in the first two experiments were chosen to match the linear L_β/T_β growth and aliquots were rejected if the L_α/T_β ratio did not fall in this range.

Samples showing a relatively high natural dose, and therefore requiring an exponential-saturating beta dose response curve (indicated as 'exp' in Table 1)

Sample Code (LV)	Sediment (Origin)	*n*	fit	$D_{e\beta}$ (Gy)	$D_{e\alpha}$ (Gy)	a-value
06	coastal, North Sea (Germany)	14	linear	2.48±0.04	-	0.023±0.002
03	coastal, North Sea (Germany)	10	linear	4.32±0.01	-	0.026±0.002
04	coastal, North Sea (Germany)	6	linear	4.37±0.02	-	0.031±0.002
104	lacustrine, (NW-England)	13	linear	2.5±0.05	-	0.028±0.002
17	coastal, North Sea (Scotland)	7	linear	23.8±0.4	-	0.027±0.002
96	loess derivate, (S-Germany)	12	linear	3.20±0.07	-	0.053±0.004
95	loess derivate, (S-Germany)	10	linear	2.84±0.06	-	0.032±0.003
97	loess derivate, (S-Germany)	6	linear	2.59±0.02	-	0.031±0.002
176	Mississippi river (N-America)	-	exp	248±43	2378±72	0.104±0.018
184	Mississippi river (N-America)	-	exp	203±14	1851±533	0.110±0.032

Table 1: *The a-values of silt-sized quartz samples analysed in this study. n indicates the number of aliquots used in the SAR protocol to calculate the a-value, fit indicates the fitting procedure used to determine the $D_{e\beta}$ of the sample (linear: y=ax+b; exp: $y = a \times (1 - e^{-\frac{x+b}{c}})$; $D_{e\beta}$ is the equivalent dose obtained from a SAR protocol using β-irradiation; $D_{e\alpha}$ is the equivalent dose obtained from a multiple aliquot additive dose (MAAD) protocol using α-irradiation.*

Sample code (LV)	*n*	Given α-dose (Gy)	Recovered ß-dose (Gy)	Recycling ratio	a-value	a-value ratio
04	6	122±8	4.02±0.17	1.03±0.03	0.033±0.002	0.94±0.08
97	6	56.8±3.7	1.76±0.06	0.97±0.02	0.031±0.002	1.00±0.09

Table 2: *The a-values of two samples determined using a dose recovery SAR protocol. A given α-dose is recovered by a SAR protocol based on ß-irradiation. The a-value ratio is the ratio between the a-value determined with the alpha irradiation at the beginning of the SAR protocol and the a-value determined with the alpha irradiation at the end of the SAR protocol.*

were measured with a multiple aliquot additive dose (MAAD) protocol. Between three and five different additive alpha doses were administered and a $D_{e\alpha}$ was determined by extrapolating the dose response curve to the dose axis. The a-value of a sample then results from the comparison of $D_{e\beta}$ and $D_{e\alpha}$.

Preheat temperatures were chosen on the basis of results from a preheat test and were 200°C, 220°C and 230°C for 10 s for low dose samples (indicated as 'linear' in Table 1) and 260°C for 10 s for high dose samples (indicated as 'exp' in Table 1). The cut heat was always 200°C, the test dose size was ~ 10% of the expected natural dose and the OSL was stimulated for 40 s at 125°C. All a-values obtained from a SAR protocol were determined as arithmetic mean and standard deviation of n values per sample (for n see Table 1 and Table 2). Assuming a normal and log-normal distribution of doses, a small number of aliquots was investigated per sample.

Results and discussion

The results of all measurements are listed in Table 1 and 2. From the first experiment, a-values ranging from 0.023 to 0.053 were determined (Table 1). Samples with linear beta dose responses gave an average a-value of 0.029±0.003 (LV96 has been excluded from this average a-value). The relative standard deviation (RSD) of 11% of this average does not originate from differences between regions, but seems to be sample-dependent as shown by LV96. The a-values of the second experiment are 0.033 and 0.041 (Table 2) and, thus, the a-value of samples with low doses seems to be independent of the measurement protocol. If the OSL-signal induced by a beta dose ($T_ß$) corrects L_α for sensitivity changes, the relationship between $T_ß$ and L_α should be proportional and the regression line should pass through the origin.

Figure 3(a) shows that the relationship is proportional for some aliquots only and that the regression line

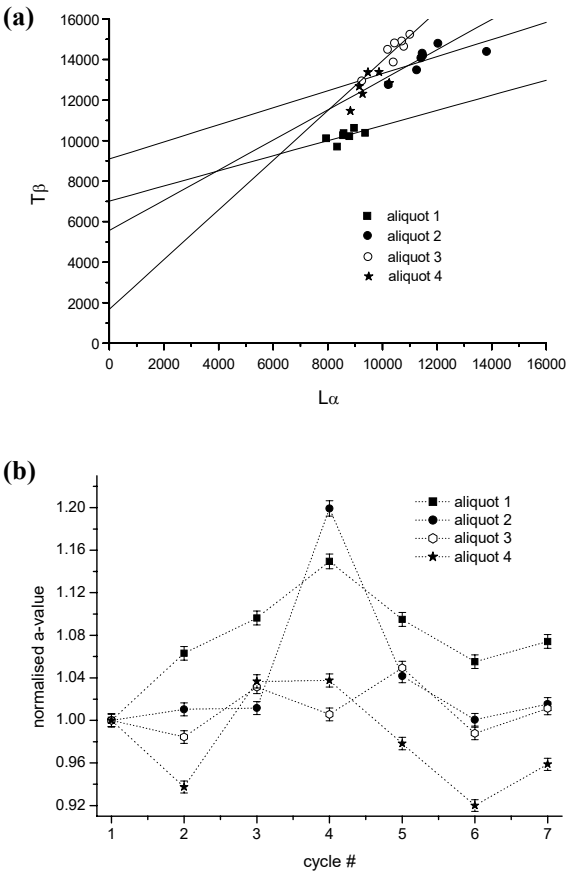

Figure 3: *Results from the sensitivity change test shown by sample LV06. Data were obtained using the protocol described in Figure 2, but using repeated alpha doses. An alpha regeneration dose of ~ 90 Gy was administered for 7 cycles (beta test dose was ~ 4 Gy). (a) Plot of T_β versus L_α; linear fitting was applied to the data set of each aliquot. (b) the a-values of the 4 aliquots of each alpha regeneration cycle normalised to the a-value of the first cycle.*

does not always pass through the origin (sample: LV06). This inter-aliquot discrepancy is reflected by the ~ 8% relative standard deviation of the SAR-derived a-values (Table 1). Moreover, Figure 3(b) shows that the a-value determined from constant alpha regeneration doses is affected by these sensitivity changes. Details plotted for one aliquot of the same sample indicate that the T_β-OSL and the L_α-OSL behave differently with each cycle (Figure 4). Sensitivity changes induced by alpha irradiation are not sufficiently monitored by the T_β-OSL and, consequently, aliquots to be used for a-value determination should be irradiated only once.

The a-value of samples showing a relatively high natural dose was determined by comparing $D_{e\beta}$ and

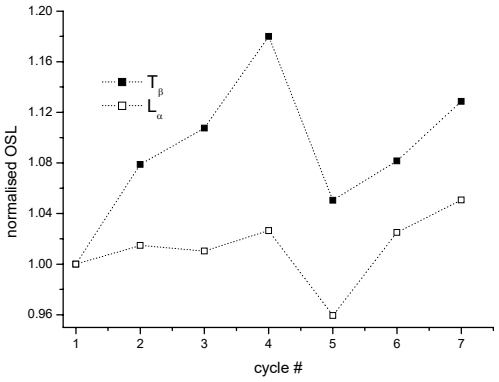

Figure 4: *Detail of the sensitivity test illustrated in Figure 3(a). L_α and T_β of aliquot 1 (LV06), normalised to the first cycle are plotted separately against cycle number.*

$D_{e\alpha}$. This comparison resulted in a-values of around 0.1 (Table 1). This value, however, is poorly constrained as it is based on the results from only two samples out of 10 samples analysed. The 8 other samples (not shown here) showed scattered dose response curves which could not be extrapolated. We believe that this is largely derived from large errors of individual dose points due to inappropriate experimental conditions (alpha source is not mounted on the luminescence reader but external). Nevertheless, the a-value of ~ 0.1 indicates that the a-value is dose-dependent. However, this result was obtained from adding charge induced by mono-energetic alpha particles to charge induced by alpha- and beta-particles and gamma photons. The different spatial distribution of charge resulting from alpha dose compared to beta and gamma radiation results in different dose response curves and, thus, this additive dose protocol is actually not accurate if the natural β-dose was relatively high. Aitken (1984) showed that the D_e is likely to be overestimated if a significant alpha dose is added to a beta dose which induced a non-linear OSL behaviour.

Conclusion

The a-values determined in this study range from 0.023 to 0.053 for samples with linear dose response. These are in agreement with a-values determined by additive dose protocols (Rees-Jones, 1995). Given the low α-effectiveness and apparent independence of sample origin, we conclude that a-values of 0.03 can be assumed for samples displaying a linear beta dose response curve allowing for an uncertainty of around 10%. With respect to the difference how alpha- and beta-particles deposit energy in silicates, comparison between regenerated alpha- and beta-doses could always be performed for low doses. We

further found in this study that sensitivity changes induced by alpha dose are not corrected by the beta dose induced test dose OSL and thus, aliquots should not be regenerated with alpha-doses but irradiated only once. The comparison between $D_{e\beta}$ and $D_{e\alpha}$ indicates that the alpha effectiveness of quartz increases with increasing dose.

References

Aitken, M. J. (1984). Non-linear growth: allowance for alpha particle contribution. *Ancient TL* **2**, 2-5.

Aitken, M. J. (1985a). *Thermoluminescence dating.* Academic Press, London

Aitken, M. (1985b). Alpha particle effectiveness: numerical relationship between systems. *Ancient TL* **3**, 22-25.

Aitken, M. J. and Bowman, S. G. E. (1975). Thermoluminescent dating: assessment of alpha particle contribution. *Archaeometry* **17**, 132-138.

Bell, W.T. (1980). Alpha dose attenuation in quartz grains for thermoluminescence dating. *Ancient TL* **12**, 4-8.

Bowman, S.G.E. and Huntley, D.J. (1984). A new proposal for the expression of alpha efficiency in TL dating. *Ancient TL* **2**, 6-8.

Brennan, B.J. and Lyons, R.G. (1989). Ranges of alpha particles in various media. *Ancient TL* **7**, 33-37.

Brennan, B.J., Lyons, R.G. and Phillips, S.W. (1991). Attenuation of alpha particle track dose for spherical grains. Nuclear Tracks *Radiation Measurements* **18**, 249-253.

Bürgi, K.A. (1992). Aufbau und Betrieb eines Thermolumineszenz-Labors zur Datierung quartärgeologischer Proben. Unpublished PhD thesis, University of Bern.

Duller, G.A.T. (2003). Distinguishing quartz and feldspar in single grain luminescence measurements. *Radiation Measurements* **37**, 161-165

Lang, A. and Wagner, G.A. (1997). Infrared stimulated luminescence dating of Holocene colluvial sediments using the 410 nm emission. *Quaternary Science Reviews* **16**, 393-396.

Lang, A., Hatté, C., Rousseau, D.-D., Antoine, P., Fontugne, M., Zöller, L. and Hambach, U. (2003). High-resolution chronologies for loess: Comparing AMS ^{14}C and optical dating results. *Quaternary Science Reviews* **22**, 953-959.

Mauz, B., Bode, T., Mainz, E., Blanchard, H., Hilger, W., Dikau, R. and Zöller, L. (2002). The luminescence dating laboratory at the University of Bonn: equipment and procedures. *Ancient TL* **20**, 53-61.

Mauz, B. and Lang, A. (2004a). Removal of the feldspar-derived luminescence component from polymineral fine silt samples for optical dating applications: evaluation of chemical treatment protocols and quality control procedures. *Ancient TL* **22**, 1-8.

Mauz, B. and Lang, A. (2004b). The dose rate of beta sources for optical dating applications: A comparison between fine silt and fine sand quartz. *Ancient TL* **22**, 45-48.

Murray, A.S. and Wintle, A. G. (2003). The single aliquot regenerative dose protocol: potential for improvements in reliability. *Radiation Measurements*, **37**, 377-381.

Rees-Jones, J. (1995). Optical dating of young sediments using fine-grain quartz. *Ancient TL*, **13**, 9-14.

Shen, Z., Mauz, B., Lang, A., Bloemendal, J., Dearing, J. (in press). Optical dating of Holocene lake sediments: Elimination of the feldspar component in fine silt quartz samples. *Quaternary Geochronology*

Singhvi, A. K. and Aitken, M. J. (1978). Americium-241 for alpha irradiations. *Ancient TL* **3**, 2-9.

Stokes, S., Ingram, S., Aitken, M.J., Sirocko, F., Anderson, R. and Leuschner, D. (2003a). Alternative chronologies for Late Quaternary (Last Interglacial-Holocene) deep sea sediments via optical dating of silt-sized quartz. *Quaternary Science Reviews* **22**, 925-941.

Stokes, S., Hetzel, R., Bailey, R.M., Mingxin, T. (2003b). Combined IRSL-OSL single aliquot regeneration (SAR) equivalent dose (D_e) estimates from source proximal Chinese loess. *Quaternary Science Reviews* **22**, 975-983.

Tribolo, C., Mercier, D. and Valladas, H. (2001). Alpha sensitivity determination in quartzite using an OSL single aliquot procedure. *Ancient TL* **19**, 47-50.

Yoshida, H., Roberts, R.G., Olley, J.M., Laslett, G.M. and Galbraith, R.F. (2000). Extending the age range of optical dating using single ‘supergrains‘ of quartz. *Radiation Measurements* **32**, 439-446.

Zimmerman, D.W. (1972). Relative thermoluminescence effects of alpha- and beta-irradiation. *Radiation Effects* **14**, 81-92.

Reviewer

Norbert Mercier

Reviewer’s Comment:

During the past two decades, only a few studies aimed at understanding how alpha particles produce luminescence in silicates, especially in quartz. This paper is a useful contribution as it confirms some previous observations and justifies the use of a mean "standard" a-value for quartz. Moreover, it shows that the effects of alpha particles are still not well understood and, consequently, the paper is an incentive for further studies.

Thesis Abstracts

Author: Lee Arnold
Thesis Title: Optical dating and computer modelling of arroyo epicycles in the American southwest
Grade: D.Phil.
Date: May 2006
Supervisors: Richard Bailey, Greg Tucker, Simon Armitage
Address: St.Peter's College, University of Oxford

The origin of arroyo cut-fill epicycles has been the subject of debate for over a century in the American southwest. Whilst it is now acknowledged that a variety of causal factors can control arroyo dynamics, there are still many outstanding research issues concerning the fundamental cause-effect relationships responsible for arroyo epicycles. This thesis aims to develop a better quantitative understanding of arroyo cut-fill dynamics and causality using a combination of optically stimulated luminescence (OSL) dating and computer modelling. The results of the chronological and modelling analyses are combined together to provide detailed reconstructions of alluvial histories within a large southern Californian arroyo system (the Cuyama River Valley) and four smaller arroyo systems located across southeastern Colorado.

An integral part of this research involves testing and demonstrating the suitability of single-grain/single-aliquot quartz OSL dating techniques in an ephemeral fluvial context. A series of simulated fluvial dose distributions and known-age empirical samples are analysed to formulate objective strategies for identifying and characterising heterogeneously bleached samples. These datasets are subsequently used to develop statistical decision procedures capable of informing the selection of appropriate 'age models' for burial dose estimation.

Computer modelling simulations conducted on a small, semi-arid ephemeral catchment demonstrate the potential for arroyo cut-fill epicycle occurrence in the absence of any precursory external climatic forcing. These modelling results provide process-based evidence for the existence of intrinsic arroyo control mechanisms and support the hypothesis that channel cutting and filling is a fundamental, natural process in ephemeral catchments. A series of additional modelling investigations are undertaken to systematically evaluate how ephemeral basins of the American southwest might have responded to climatic events during the late Quaternary. These sensitivity tests demonstrate that it is too simplistic to conceptualise arroyo epicycles in terms of mean precipitation shifts; the key to understanding arroyo behaviour from a climatic perspective lies with a more complete consideration of individual climatic parameters such as rainfall intensity, frequency, duration and seasonality.

The complex relationship between climate change and arroyo formation is particularly evident in the reconstructed alluvial histories of the southeastern Colorado arroyo systems. In the Cuyama River Valley, climate appears to have controlled arroyo dynamics both directly and indirectly through a complex interplay with, and conditioning of, hydrology, hillslope processes and vegetation dynamics.

Author: George S. Polymeris
Thesis Title: Low dose detection by thermoluminescence and optically stimulated luminescence using minerals as time integrating luminescence dosimeters
Grade: PhD
Date: June 2006
Supervisors: George Kitis
Address: Aristotle University of Thessaloniki, Physics Department, Nuclear Physics Laboratory, GR – 54124, Thessaloniki, Greece
&
Cultural and Educational Technology Institute (C.E.T.I.), Research Centre "ATHENA", Tsimiski 58, GR – 67100, Xanthi, Greece.

The present thesis investigates whether certain geological natural minerals, such as quartz (SiO_2) and/or natural calcium fluoride (CaF_2:N), could be effectively used as Time – Integrating Luminescence Detectors for setting bounds on interaction's strength

of dark matter particles with ordinary matter. The limitations imposed by the background of cosmic radiation as well as environmental radioactivity are investigated, and initial limits for the interaction strengths with ordinary matter, and the mass of Weakly Interacting Massive Particles (WIMPs) and axions are derived. The Optically Stimulated Luminescence (OSL) properties of the natural calcium fluoride are studied, indicating it as the most suitable phosphor, for the proposed method, mainly due to its extremely low detectable dose threshold. The effective application of the retrospective dosimetry's working principle in deep sea sediments is also indicated, using a deep sea sediment core collected from the operational site of the NESTOR experiment, 14 km off the South – West Coast of Peloponnesus, at a depth of almost 4 km. Therefore, the use of quartz from deep sea sediments is proposed as well, mainly due to the shielding provided by water from cosmic rays. Finally, the possibility of using the pre-dose technique protocol in the OSL signal is studied by taking advantage of the sensitization of its second component.

Author: Kira Westaway
Thesis Title: Reconstructing the Quaternary landscape evolution and climate history of western Flores: an environmental and chronological context for an archaeological site
Grade: PhD.
Date: September 2006
Supervisors: Richard Roberts
Address: University of Wollongong, New South Wales, Australia

The recent discovery of a late-surviving new human species, *Homo floresiensis*, in western Flores has accentuated our lack of understanding of the history of the genus *Homo* in Asia and of the environmental challenges that may have influenced these hominins. Western Flores contains a wealth of archaeological and palaeoanthropological material with far-reaching implications for human evolution and for Indonesian, Australian and world archaeology. But the interpretation of this evidence has been hindered by a limited Quaternary context and age control for complex stratigraphies in a region of great geological instability and widespread environmental change.

Liang Bua in western Flores is a key site in the Indonesian archaeological record, providing evidence of cave occupation by *Homo floresiensis* and *Homo sapiens*, and human evolution and dispersal on the eastern side of Wallace's Line. In this study, archaeologically-relevant information has been gleaned from an interdisciplinary approach to the analysis of this site, and has established the timing of key events, such as the first exposure of the cave and the nature of, and influences on, human occupation of the cave. This approach incorporated studies of landscape evolution, river terrace and cave development, sedimentology of cave sediments, palaeoclimate signals in speleothems, and a dating strategy utilising novel approaches to luminescence dating.

The research reported here provides a chronological and environmental backdrop to the human occupation of Liang Bua. A maximum age of cave occupation is shown to correspond to the time of cave exposure (~190 ka), which also represents a minimum age for the human habitation of the area. In addition, this study has established an age range for the occupation of the cave by *Homo floresiensis* (95–11 ka), the time of the most intensive phases of occupation (74–61 and 17–11 ka), the depositional age of the holotype skeleton (36–14 ka), and the age of the oldest human skeletal remains found on Flores (95–74 ka). Through the integration of techniques, a framework for terrace development and landscape evolution has been developed to establish the Quaternary setting in which the cave was formed and evolved. These techniques have also defined a sequence of geomorphological and sedimentological changes in the cave, enabling the reconstruction of the occupational environment. At least two zones of occupation have been identified: a zone established ~74–61 ka, and a later zone established ~18 ka.

The environmental backdrop for the arrival and dispersal of humans throughout Indonesia has been established via a palaeoclimatic and palaeoenvironmental analysis of speleothem records. These records contain evidence of multiple wet phases (110–98, 82–65, 49–39 and 17–5 ka) and a flourishing fauna. The timing of these wet phases correlate with evidence for channel and flowstone formation, episodic erosion events, and the most intensive periods of occupation in the cave. There is also evidence for a prolonged period of reduced rainfall (36–17 ka) in an organic-poor environment, the timing of which correlates with evidence of reduced erosion, pooling and less intense occupation. These correlations suggest that the occupational success of *Homo floresiensis* in this area was related to the contemporaneous environmental conditions, which, combined with the evidence for at least two volcanic events (one of which may have forced

human migration), establish a link between hominids and their environment.

The results of this research indicate the value of using an interdisciplinary approach to investigate and interpret archaeological sites in Southeast Asia. By providing an environmental and chronological context for important archaeological finds, we can develop a better understanding of the prehistory of *Homo* in Asia.

Bibliography
Compiled by Ann Wintle

From 1st June 2006 to 1st October 2006

Bailey, R. M., and Arnold, L. J. (2006). Statistical modelling of single grain quartz D_e distributions and an assessment of procedures for estimating burial dose. *Quaternary Science Reviews* **25,** 2475-2502.

Bateman, M. D., and Murton, J. B. (2006). The chronostratigraphy of Late Pleistocene glacial and periglacial aeolian activity in the Tuktoyaktuk Coastlands, NWT, Canada. *Quaternary Science Reviews* **25,** 2552-2568.

Beerten, K., Lomax, J., Clemer, K., Stesmans, A., and Radtke, U. (2006). On the use of Ti centres for estimating burial ages of Pleistocene sedimentary quartz: Multiple-grain data from Australia. *Quaternary Geochronology* **1,** 151-158.

Berger, G. W. (2006). Trans-arctic-ocean tests of fine-silt luminescence sediment dating provide a basis for an additional geochronometer for this region. *Quaternary Science Reviews* **25,** 2529-2551.

Briant, R. M., Bates, M. R., Schwenninger, J. L., and Wenban-Smith, F. (2006). An optically stimulated luminescence dated Middle to Late Pleistocene fluvial sequence from the western Solent Basin, southern England. *Journal of Quaternary Science* **21,** 507-523.

Bristow, C. S., and Pucillo, K. (2006). Quantifying rates of coastal progradation from sediment volume using GPR and OSL: the Holocene fill of Guichen Bay, south-east South Australia. *Sedimentology* **53,** 769-788.

Carr, A. S., Thomas, D. S. G., Bateman, M. D., Meadows, M. E., and Chase, B. (2006). Late Quaternary palaeoenvironments of the winter-rainfall zone of southern Africa: Palynological and sedimentological evidence from the Agulhas Plain. *Palaeogeography Palaeoclimatology Palaeoecology* **239,** 147-165.

Choi, J. H., Murray, A. S., Cheong, C. S., Hong, D. G., and Chang, H. W. (2006). Estimation of equivalent dose using quartz isothermal TL and the SAR procedure. *Quaternary Geochronology* **1,** 101-108.

Chruscinska, A. (2006). Modelling the optical bleaching of a complex TL signal. *Journal of Physics D-Applied Physics* **39,** 2321-2329.

Clemmensen, L. B., and Murray, A. (2006). The termination of the last major phase of aeolian sand movement, coastal dunefields, Denmark. *Earth Surface Processes and Landforms* **31,** 795-808.

Cooper, A. F., and Kostro, F. (2006). A tectonically uplifted marine shoreline deposit, Knights Point, Westland, New Zealand. *New Zealand Journal of Geology and Geophysics* **49,** 203-216.

Cordier, S., Harmand, D., Frechen, M., and Beiner, M. (2006). Fluvial system response to Middle and Upper Pleistocene climate change in the Meurthe and Moselle valleys (Eastern Paris Basin and Rhenish Massif). *Quaternary Science Reviews* **25,** 1460-1474.

Correcher, V., Sanchez-Munoz, L., Garcia-Guinea, J., Gomez-Ros, J. M., and Delgado, A. (2006). On the blue thermoluminescence emission of synthetic Li-rich aluminosilicates. *Nuclear Instruments & Methods in Physics Research A* **562,** 456-460.

Cruz-Zaragoza, E., Furetta, C., Kitis, G., Gomez, B. T., Polymeris, G. S., Tsirliganis, N., and Loukou, Z. (2006). Thermoluminescence characterization of the irradiated minerals extracted from nopal. *Radiation Effects and Defects in Solids* **161,** 267-278.

Cupper, M. L. (2006). Luminescence and radiocarbon chronologies of playa sedimentation in the Murray Basin, southeastern Australia. *Quaternary Science Reviews* **25,** 2594-2607.

Dantas, S. C., Valerio, M. E. G., dos Santos, M. A. C., and Souza, D. D. N. (2006). Photoinduced emission and thermoluminescence in topaz. *Nuclear Instruments & Methods in Physics Research Section B* **250,** 386-389.

De Corte, F., Vandenberghe, D., Buylaert, J. P., Van den haute, P., and Kucera, J. (2006). Relative and k_0-standardized INAA to assess the internal (Th, U) radiation dose rate in the "quartz coarse-grain protocol" for OSL dating of sediments: Unexpected observations. *Nuclear Instruments and Methods in Physics Research Section A* **564,** 743-751.

Despriee, J., Gageonnet, R., Voinchet, P., Bahain, J.-J., Falgueres, C., Varache, F., Courcimault, G., and Dolo, J.-M. (2006). Une occupation humaine au Pleistocene inferieur sur la bordure nord du Massif central. *Comptes Rendus Palevol* **5,** 821-828.

Duller, G. A. T., and Augustinus, P. C. (2006). Reassessment of the record of linear dune activity in Tasmania using optical dating. *Quaternary Science Reviews* **25,** 2608-2618.

Eiriksson, J., Kristensen, P. H., Lykke-Andersen, H., Brooks, K., Murray, A., Knudsen, K. L., and Glaister, C. (2006). A sedimentary record from a deep Quaternary valley in the southern Lillebaelt area, Denmark: Eemian and Early Weichselian lithology and chronology at Mommark. *Boreas* **35,** 320-331.

Fattahi, M., Singarayer, J.S., Bailey, R.M. and Stokes, S. (2006). The linearly modulated IRSL red emission from feldspars. *Geochronometria* **25**, 19-28.

Fattahi, M., Walker, R., Hollingsworth, J., Bahroudi, A., Nazari, H., Talebian, M., Armitage, S., and Stokes, S. (2006). Holocene slip-rate on the Sabzevar thrust fault, NE Iran, determined using optically stimulated luminescence (OSL). *Earth and Planetary Science Letters* **245,** 673-684.

Favalli, A., Furetta, C., Zaragoza, E. C., and Reyes, A. (2006). Computerized glow curve deconvolution of thermoluminescent emission from polyminerals of Jamaica Mexican flower. *Radiation Effects and Defects in Solids* **161,** 591-602.

Feathers, J. K., Holliday, V. T., and Meltzer, D. J. (2006). Optically stimulated luminescence dating of Southern High Plains archaeological sites. *Journal of Archaeological Science* **33,** 1651-1665.

Fedorowicz, S. (2006). TL age of Upper Pleistocene stratified deposits measured using the additive, regeneration and R Gamma methods. *Geological Quarterly* **50,** 211-218.

Forman, S. L., Spaeth, M., Marin, L., Pierson, J., Gomez, J., Bunch, F., and Valdez, A. (2006). Episodic Late Holocene dune movements on the sand-sheet area, Great Sand Dunes National Park and Preserve, San Luis Valley, Colorado, USA. *Quaternary Research* **66,** 97-108.

Galli, A., Poldi, G., Martini, M., Sibilia, E., Montanari, C., and Panzeri, L. (2006). Study of blue colour in ancient mosaic tesserae by means of thermoluminescence and reflectance measurements. *Applied Physics* **83,** 675-679.

Gardner, T. W., Webb, J., Davis, A. G., Cassel, E. J., Pezzia, C., Merritts, D. J., and Smith, B. (2006). Late Pleistocene landscape response to climate change: eolian and alluvial fan deposition, Cape Liptrap, southeastern Australia. *Quaternary Science Reviews* **25,** 1552-1569.

Göksu, H. Y., Stepanenko, V. F., Bailiff, I. K., and Jungner, H. (2006). Intercomparison of luminescence measurements of bricks from Dolon' village: Experimental methodology and results of European study group. *Journal of Radiation Research* **47,** A29-A37.

Gong, G., Xia, B., and Liu, S. (2006). Study on feldspar thermoluminescence spectra and its luminescence dating implication. *Nuclear Instruments and Methods in Physics Research, Section B* **251,** 143-147.

Greenbaum, N., Porat, N., Rhodes, E., and Enzel, Y. (2006). Large floods during late Oxygen Isotope Stage 3, southern Negev desert, Israel. *Quaternary Science Reviews* **25,** 704-719.

Greilich, S., Harney, H. L., Woda, C., and Wagner, G. A. (2006). AgesGalore--A software program for evaluating spatially resolved luminescence data. *Radiation Measurements* **41,** 726-735.

Grün, R. (2006). A simple method for the rapid assessment of the qualitative ESR response of fossil samples to laboratory irradiation. *Radiation Measurements* **41,** 682-689.

Grün, R., Eggins, S., Wells, R. T., Rhodes, E., Bestland, E., Spooner, N., Ayling, M., Forbes, M., and McCulloch, M. (2006). A cautionary tale from down under: Dating the BlackCreek Swamp megafauna site on Kangaroo Island, South Australia. *Quaternary Geochronology* **1,** 142-150.

Hanson, P. R., Mason, J. A., and Goble, R. J. (2006). Fluvial terrace formation along Wyoming's Laramie Range as a response to increased late Pleistocene flood magnitudes. *Geomorphology* **76,** 12-25.

Hashimoto, T., Yamaguchi, T., Tajika, Y., Takeuchi, A., and Yawata, T. (2006). Behavior of TL glowcurves for natural quartz samples from liquid-nitrogen temperature up to room temperature. *Radiation Measurements* **41,** 671-676.

Hawke, R. M., and McConchie, J. A. (2006). Dune phases in the Otaki-Te Horo area (New Zealand): a geomorphic history. *Earth Surface Processes and Landforms* **31,** 633-645.

Huang, C. C., Pang, J. L., Chen, S. E., Su, H. X., Han, J., Cao, Y. F., Zhao, W. Y., and Tan, Z. H. (2006). Charcoal records of fire history in the Holocene loess-soil sequences over the southern Loess Plateau of China. *Palaeogeography Palaeoclimatology Palaeoecology* **239,** 28-44.

Huntley, D. J., and Lian, O. B. (2006). Some observations on tunnelling of trapped electrons in feldspars and their implications for optical dating. *Quaternary Science Reviews* **25,** 2503-2512.

Jacobs, Z., Duller, G. A. T., Wintle, A. G., and Henshilwood, C. S. (2006). Extending the chronology of deposits at Blombos Cave, South Africa, back to 140 ka using optical dating of single and multiple grains of quartz. *Journal of Human Evolution* **51,** 255-273.

Jacobs, Z., Wintle, A. G., and Duller, G. (2006). Evaluation of SAR procedures for D_e determination using single aliquots of quartz from two archaeological sites in South Africa. *Radiation Measurements* **41,** 520-533.

Juyal, N., Chamyal, L. S., Bhandari, S., Bhushan, R., and Singhvi, A. K. (2006). Continental record of the southwest monsoon during the last 130 ka: evidence from the southern margin of the Thar Desert, India. *Quaternary Science Reviews* **25,** 2632-2650.

Kadereit, A., Dehner, U., Hansen, L., Pare, C., and Wagner, G. A. (2006). Geoarchaeological studies of man-environment interaction at the Glauberg, Wetterau, Germany. *Zeitschrift für Geomorphologie* **142,** 109-133.

Kadereit, A., Sponholz, B., Rösch, M., Schier, W., Kromer, B., and Wagner, G. A. (2006). Chronology of Holocene environmental changes at the tell site of Uivar, Romania, and its significance for late Neolithic tell evolution in the temperate Balkans. *Zeitschrift für Geomorphologie* **142,** 19-45.

Kaiser, K., Miehe, G., Schoch, W. H., Zander, A., and Schlütz, F. (2006). Relief. soil and lost forests: Late Holocene environmental changes in southern Tibet under human impact. *Zeitschrift für Geomorphologie* **142,** 149-173.

Kalm, V. (2006). Pleistocene chronostratigraphy in Estonia, southeastern sector of the Scandinavian glaciation. *Quaternary Science Reviews* **25,** 960-975.

Kemp, R. A., Zarate, M., Toms, P., King, M., Sanabria, J., and Arguello, G. (2006). Late Quaternary paleosols, stratigraphy and landscape evolution in the Northern Pampa, Argentina. *Quaternary Research* **66,** 119-132.

Kitazawa, T., Nakagawa, T., Hashimoto, T., and Tateishi, M. (2006). Stratigraphy and optically stimulated luminescence (OSL) dating of a Quaternary sequence along the Dong Nai River, southern Vietnam. *Journal of Asian Earth Sciences* **27,** 788-804.

Krull, E. S., Bestland, E. A., Skjemstad, J. O., and Parr, J. F. (2006). Geochemistry (delta C-13, delta N-15, C-13 NMR) and residence times (C-14 and OSL) of soil organic matter from red-brown earths of South Australia: Implications for soil genesis. *Geoderma* **132,** 344-360.

Lai, Z. P., and Wintle, A. G. (2006). Locating the boundary between the Pleistocene and the Holocene in Chinese loess using luminescence. *The Holocene* **16,** 893-899.

Lang, A., and Mauz, B. (2006). Towards chronologies of gully formation: optical dating of gully fill sediments from Central Europe. *Quaternary Science Reviews* **25,** 2666-2675.

Larsen, E., Kjaer, K. H., Jensen, M., Demidov, I. N., Hakansson, L., and Paus, A. (2006). Early Weichselian palaeoenvironments reconstructed from a mega-scale thrust-fault complex, Kanin Peninsula, northwestern Russia. *Boreas* **35,** 476-492.

Leth, T., Hansen, H. B., and Boisen, F. (2006). Comparison of three methods for detection of herbal food supplement irradiation. *European Food Research and Technology* **223,** 39-43.

Li, B., and Li, S. H. (2006). Studies of thermal stability of charges associated with thermal transfer of OSL from quartz. *Journal of Physics D-Applied Physics* **39,** 2941-2949.

Li, B., Li, S.-H., and Wintle, A. G. (2006). Observations of thermal transfer and the slow component of OSL signals from quartz. *Radiation Measurements* **41,** 639-648.

Li, S. H., and Li, B. (2006). Dose measurement using the fast component of LM-OSL signals from quartz. *Radiation Measurements* **41,** 534-541.

Li, S. H., and Yin, G. M. (2006). Luminescence properties of biotite relevant to dating and dosimetry. *Journal of Luminescence* **121,** 51-56.

Lian, O. B., and Roberts, R. G. (2006). Dating the Quaternary: progress in luminescence dating of sediments. *Quaternary Science Reviews* **25,** 2449-2468.

Lu, H., Stevens, T., Yi, S., and Sun, X. (2006). An erosional hiatus in Chinese loess sequences revealed by closely spaced optical dating. *Chinese Science Bulletin* **51,** 2253-2259.

Machalett, B., Frechen, M., Hambach, U., Oches, E. A., Zoller, L., and Markovic, S. B. (2006). The loess sequence from Remisowka (northern boundary of the Tien Shan Mountains, Kazakhstan) - Part I: Luminescence dating. *Quaternary International* **152,** 192-201.

Machtle, B., Eitel, B., Kadereit, A., and Unkel, I. (2006). Holocene environmental changes in the northern Atacama desert, Southern Peru (14°30' S) and their impact on the rise and fall of pre-Columbian cultures. *Zeitschrift für Geomorphologie* **142,** 47-62.

Mange, M. A., and Otvos, E. G. (2005). Gulf coastal plain evolution in West Louisiana: Heavy mineral provenance and Pleistocene alluvial chronology. *Sedimentary Geology* **182,** 29-57.

Mathew, G., Singhvi, A. K., and Karanth, R. V. (2006). Luminescence chronometry and geomorphic evidence of active fold growth along the Kachchh Mainland Fault (KMF), Kachchh, India: Seismotectonic implications. *Tectonophysics* **422,** 71-87.

Millard, A. R. (2006). Bayesian analysis of ESR dates, with application to Border Cave. *Quaternary Geochronology* **1,** 159-166.

Millard, A. R. (2006). Bayesian analysis of Pleistocene chronometric methods. *Archaeometry* **48,** 359-375.

Mischke, S., Herzschuh, U., Sun, N. D., Qiao, Z. Z., and Sun, Z. C. (2006). A large Middle Pleistocene freshwater to oligohaline lake in the contemporary hyperarid Qaidam Basin (China). *Episodes* **29,** 34-38.

Mischke, S., Herzschuh, U., Sun, Z. C., Qiao, Z. Z., Sun, N. D., and Zander, A. M. (2006). Middle Pleistocene Ostracoda from a large freshwater lake in the presently dry Qaidam Basin (NW China). *Journal of Micropalaeontology* **25,** 57-64.

Molodkov, A., and Bitinas, A. (2006). Sedimentary record and luminescence chronology of the Lateglacial and Holocene aeolian sediments in Lithuania. *Boreas* **35,** 244-254.

Molodkov, A. N., and Bolikhovskaya, N. S. (2006). Long-term palaeoenvironmental changes recorded in palynologically studied loess-palaeosol and ESR-dated marine deposits of Northern Eurasia: Implications for sea-land correlation. *Quaternary International* **152-153,** 48-58.

Ogundare, F. O., and Chithambo, M. L. (2006). Two-point method for kinetic analysis of a thermoluminescence glow peak. *Radiation Effects and Defects in Solids* **161,** 289-296.

Ogundare, F. O., Chithambo, M. L., and Oniya, E. O. (2006). Anomalous behaviour of thermoluminescence from quartz: A case of glow peaks from a Nigerian quartz. *Radiation Measurements* **41,** 549-553.

Ogundare, F. O., Mokobia, C. E., and Balogun, F. A. (2006). Kinetic study of the thermoluminescence glow curve of natural dolerite. *Radiation Effects and Defects in Solids* **161,** 395-400.

Olley, J. M., Roberts, R. G., Yoshida, H., and Bowler, J. M. (2006). Single-grain optical dating of grave-infill associated with human burials at Lake Mungo, Australia. *Quaternary Science Reviews* **25,** 2469-2474.

Owen, L. A., Finkel, R. C., Haizhou, M., and Barnard, P. L. (2006). Late Quaternary landscape evolution in the Kunlun Mountains and Qaidam Basin, Northern Tibet: A framework for examining the links between glaciation, lake level changes and alluvial fan formation. *Quaternary International* **154-155,** 73-86.

Pant, R. K., Juyal, N., Basavaiah, N., and Singhvi, A. K. (2006). Late Quaternary glaciation and seismicity in the Higher Central Himalaya: Evidence from Shalang basin (Goriganga), Uttaranchal. *Current Science* **90,** 1500-1505.

Pederson, J. L., Anders, M. D., Rittenour, T. M., Sharp, W. D., Gosse, J. C., and Karlstrom, K. E. (2006). Using fill terraces to understand incision rates and evolution of the Colorado River in eastern Grand Canyon, Arizona. *Journal of Geophysical Research-Earth Surface* **111**.

Pedoja, K., Ortheb, L., Dumont, J. F., Lamothe, M., Ghaleb, B., Auclair, M., and Labrousse, B. (2006). Quaternary coastal uplift along the Talara Arc (Ecuador, Northern Peru) from new marine terrace data. *Marine Geology* **228,** 73-91.

Pei, S. W., Zhang, J. F., Gao, X., Zhou, L. P., Feng, X. W., and Chen, F. Y. (2006). Optical dating of the Jingshuiwan Paleolithic site of Three Gorges, China. *Chinese Science Bulletin* **51,** 1334-1342.

Polymeris, G. S., Kitis, G., Liolios, A. K., Tsirliganis, N. C., and Zioutas, K. (2006). Minerals as Time-Integrating Luminescence Detectors for setting bounds on dark matter particle characteristics. *Nuclear Instruments & Methods in Physics Research Section A* **562,** 207-213.

Poolton, N. R. J., Mauz, B., Lang, A., Jain, M., and Malins, A. E. R. (2006). Optical excitation processes in the near band-edge region of KAlSi3O8 and NaAlSi3O8 feldspar. *Radiation Measurements* **41,** 542-548.

Porat, N., Rosen, S. A., Boaretto, E., and Avni, Y. (2006). Dating the Ramat Saharonim Late Neolithic desert cult site. *Journal of Archaeological Science* **33,** 1341-1355.

Poreba, G., Moska, P., and Bluszcz, A. (2006). On the contribution of radioactive fallout isotopes to the total dose rate in dating of young sediments. *Geochronometria* **25,** 47-50.

Prakash, J., Singh, P. K., and Dwivedi, D. K. (2006). Thermally stimulated processes: I-Mechanisms involved in the appearance of a thermoluminescence glow curve. *Indian Journal of Pure & Applied Physics* **44,** 532-536.

Puchalska, M., and Bilski, P. (2006). GlowFit--a new tool for thermoluminescence glow-curve deconvolution. *Radiation Measurements* **41,** 659-664.

Quigley, M. C., Cupper, M. L., and Sandiford, M. (2006). Quaternary faults of south-central Australia: palaeoseismicity, slip rates and origin. *Australian Journal of Earth Sciences* **53,** 285-301.

Ramzaev, V., and Goksu, H. Y. (2006). Cumulative dose assessment using thermoluminescence properties of porcelain isolators as evidence of a severe radiation accident in the Republic of Sakha (Yakutia), Russia, 1978. *Health Physics* **91,** 263-269.

Rasheedy, M. S., El-Sherif, M. A., and Hefni, M. A. (2006). Applications of the three points analysis method for obtaining the trap parameters and the separation of thermoluminescence glow curve into its components. *Radiation Effects and Defects in Solids* **161,** 579-590.

Rhodes, E. J., Singarayer, J. S., Raynal, J. P., Westaway, K. E., and Sbihi-Alaoui, F. Z. (2006). New age estimates for the Palaeolithic assemblages and Pleistocene succession of Casablanca, Morocco. *Quaternary Science Reviews* **25,** 2569-2585.

Robertson, G. B., and Prescott, J. R. (2006). Luminescence dating at the archaeological and human burial site at Roonka, South Australia. *Quaternary Science Reviews* **25,** 2586-2593.

Robinson, R. A. J., Spencer, J. Q. G., Strecker, M. R., Richter, A., and Alonso, R. N. (2005). Luminescence dating of alluvial fans in intramontane basins of NW Argentina. *Geological Society Special Publication* **251,** 153-168.

Rodnight, H., Duller, G. A. T., Wintle, A. G., and Tooth, S. (2006). Assessing the reproducibility and accuracy of optical dating of fluvial deposits. *Quaternary Geochronology* **1,** 109-120.

Sadlo, J., Michalik, J., Stachowicz, W., Strzelczak, G., Dziedzic-Goclawska, A., and Ostrowski, K. (2006). EPR study on biominerals as materials for retrospective dosimetry. *Nukleonika* **51,** S95-S100.

Sanchez-Munoz, L., Garcia-Guinea, J., Sanz, J., Correcher, V., and Delgado, A. (2006). Ultraviolet luminescence from defect complexes in the twin boundaries of K-feldspar. *Chemistry of Materials* **18,** 3336-3342.

Soliman, C., and Metwally, S. M. (2006). Thermoluminescence of the green emission band of calcite. *Radiation Effects and Defects in Solids* **161,** 607-613.

Souza, D. N., de Lima, J. F., Valerio, M. E. G., and Caldas, L. V. E. (2006). Thermally stimulated luminescence and EPR studies on topaz. *Applied Radiation and Isotopes* **64,** 906-909.

Srivastava, P., Brook, G. A., Marais, E., Morthekai, P., and Singhvi, A. K. (2006). Depositional environment and OSL chronology of the Homeb silt deposits, Kuiseb River, Namibia. *Quaternary Research* **65,** 478-491.

Stevens, T., Armitage, S. J., Lu, H. Y., and Thomas, D. S. G. (2006). Sedimentation and diagenesis of Chinese loess: implications for the preservation of continuous, high-resolution climate records. *Geology* **34,** 849-852.

Stone, T. (2006). Last glacial cycle hydrological change at Lake Tyrrell, southeast Australia. *Quaternary Research* **66,** 176-181.

Stone, T. (2006). The late-Holocene origin of the modern Murray River course, southeastern Australia. *Holocene* **16,** 771-778.

Telfer, M. W., and Thomas, D. S. G. (2006). Complex Holocene lunette dune development, South Africa: implications for paleoclimate and models of pan development. *Geology* **34,** 853-856.

Thomas, P. J., Murray, A. S., Kjaer, K. H., Funder, S., and Larsen, E. (2006). Optically Stimulated Luminescence (OSL) dating of glacial sediments from Arctic Russia - depositional bleaching and methodological aspects. *Boreas* **35,** 587-599.

Turkin, A. A., Vainshtein, D. I., and Den Hartog, H. W. (2006). Modelling of optically stimulated luminescence of zircon: assessment of the suitability for dating. *Journal of Physics D-Applied Physics* **39,** 1367-1377.

Wang, W. D., Xia, J. D., and Zhou, Z. X. (2006). Thermoluminescence dating of the ancient Chinese porcelain using a regression method of saturation exponential in pre-dose technique. *Science in China Series E-Technological Sciences* **49,** 194-209.

Wang, X., and Miao, X. (2006). Weathering history indicated by the luminescence emissions in Chinese loess and paleosol. *Quaternary Science Reviews* **25,** 1719-1726.

Wang, X. L., Lu, Y. C., and Wintle, A. G. (2006). Recuperated OSL dating of fine-grained quartz in Chinese loess. *Quaternary Geochronology* **1,** 89-100.

Wang, X. L., Wintle, A. G., and Lu, Y. C. (2006). Thermally transferred luminescence in fine-grained quartz from Chinese loess: Basic observations. *Radiation Measurements* **41,** 649-658.

Westaway, K. E., and Roberts, R. G. (2006). A dual-aliquot regenerative-dose protocol (DAP) for thermoluminescence (TL) dating of quartz sediments using the light-sensitive and isothermally stimulated red emissions. *Quaternary Science Reviews* **25,** 2513-2528.

Williams, M., Talbot, M., Aharon, P., Abdl Salaam, Y., Williams, F., and Inge Brendeland, K. (2006). Abrupt return of the summer monsoon 15,000 years ago: new supporting evidence from the lower White Nile valley and Lake Albert. *Quaternary Science Reviews* **25,** 2651-2665.

Williams, M. A. J., Pal, J. N., Jaiswal, M., and Singhvi, A. K. (2006). River response to Quaternary climatic fluctuations: evidence from the Son and Belan valleys, north-central India. *Quaternary Science Reviews* **25,** 2619-2631.

Xu, Z., Zhang, F. J., Zhao, S. L., Wang, L. W., Georgobiani, A. N., Gutan, V. B., and Meng, L. J. (2006). Simultaneous determination of trap depth and the ratio of the rate of recombination to that of capture from thermo-luminescence. *Chinese Physics* **15,** 1883-1887.

Yang, X. P., Preusser, F., and Radtke, U. (2006). Late Quaternary environmental changes in the Taklamakan Desert, western China, inferred from OSL-dated lacustrine and aeolian deposits. *Quaternary Science Reviews* **25,** 923-932.

Yazici, A. N., Kurt, K., Kafadar, V. E., Gurler, S., and Topaksu, M. (2006). The analysis of thermolurninescent glow peaks of natural zircon after beta-irradiation. *Nuclear Instruments & Methods in Physics Research Section B* **248,** 133-141.

Zacharias, N., Michael, C. T., Georgakopolou, M., Kilikoglou, V., and Bassiakos, Y. (2006). Quartz TL dating on selected layers from archaeometallurgical kiln fragments: a proposed procedure to overcome age dispersion. *Geochronometria* **25,** 29-35.

Zahedifar, M., Karimi, L., and Kavianinia, M. J. (2006). Thermoluminescence general-order glow curve deconvolution function with continuous distribution of activation energies. *Nuclear Instruments & Methods in Physics Research Section A* **564,** 515-520.

Zhang, H. C., Ming, Q. Z., Lei, G. L., Zhang, W. X., Fan, H. F., Chang, F. Q., Wunnemann, B., and Hartmann, K. (2006). Dilemma of dating on lacustrine deposits in an hyperarid inland basin of NW China. *Radiocarbon* **48,** 219-226.

LED2005 published papers in Radiation Measurements (Aug-Sept 2006)

Adamiec, G., Bluszcz, A., Bailey, R., and Garcia-Talavera, M. (2006). Finding model parameters: Genetic algorithms and the numerical modelling of quartz luminescence. *Radiation Measurements* **41**, 897-902.

Ankjaergaard, C., Murray, A. S., Denby, P. M., and Botter-Jensen, L. (2006). Measurement of optically and thermally stimulated electron emission from natural minerals. *Radiation Measurements* **41**, 780-786.

Bailiff, I. K. (2006). Development of single grain OSL dating of ceramic materials: Spatially resolved measurement of absorbed dose. *Radiation Measurements* **41**, 744-749.

Baly, L., Quesada, I., Otazo, M. R., Ramos, M., and Gonzalez, Y. (2006). Influence of non-uniformity of the stimulation source on quartz OSL signals. *Radiation Measurements* **41**, 787-789.

Bassinet, C., Mercier, N., Miallier, D., Pilleyre, T., Sanzelle, S., and Valladas, H. (2006). Thermoluminescence of heated quartz grains: Intercomparisons between SAR and multiple-aliquot additive dose techniques. *Radiation Measurements* **41**, 803-808.

Bitencourt, J. F. S., Silva, D. M., Silva, P. H., Kinoshita, A., Munita, C. S., and Tatumi, S. H. (2006). Luminescence and ESR properties of Brazilian feldspars. *Radiation Measurements* **41**, 948-953.

Bluszcz, A., and Adamiec, G. (2006). Application of differential evolution to fitting OSL decay curves. *Radiation Measurements* **41**, 886-891.

Bos, A. J. J., Wallinga, J., Johns, C., Abellon, R. D., Brouwer, J. C., Schaart, D. R., and Murray, A. S. (2006). Accurate calibration of a laboratory beta particle dose rate for dating purposes. *Radiation Measurements* **41**, 1020-1025.

Brennan, B. J. (2006). Variation of the alpha dose rate to grains in heterogeneous sediments. *Radiation Measurements* **41**, 1026-1031.

Chithambo, M. L. (2006). On the correlation between annealing and variabilities in pulsed-luminescence from quartz. *Radiation Measurements* **41**, 862-865.

Choi, J. H., Duller, G. A. T., Wintle, A. G., and Cheong, C. S. (2006). Luminescence characteristics of quartz from the Southern Kenyan Rift Valley: Dose estimation using LM-OSL SAR. *Radiation Measurements* **41**, 847-854.

Correcher, V., Garcia-Guinea, J., Castillejo, M., Oujja, M., Rebollar, E., and Lopez-Arce, P. (2006). Laser-induced fluorescence and thermoluminescence response of a Na-Ca rich silicate. *Radiation Measurements* **41**, 971-975.

Cosma, C., Benea, V., Timar, A., Barbos, D., and Paunoiu, C. (2006). Preliminary dating results for ancient ceramics from Romania by means of thermoluminescence. *Radiation Measurements* **41**, 987-990.

Denby, P. M., Botter-Jensen, L., Murray, A. S., Thomsen, K. J., and Moska, P. (2006). Application of pulsed OSL to the separation of the luminescence components from a mixed quartz/feldspar sample. *Radiation Measurements* **41**, 774-779.

Galli, A., Martini, M., Montanari, C., Panzeri, L., and Sibilia, E. (2006). TL of fine-grain samples from quartz-rich archaeological ceramics: Dosimetry using the 110 and TL peaks. *Radiation Measurements* **41**, 1009-1014.

Godfrey-Smith, D. I. (2006). Applicability of moissanite, a monocrystalline form of silicon carbide to retrospective and forensic dosimetry. *Radiation Measurements* **41**, 976-981.

Greilich, S., and Wagner, G. A. (2006). Development of a spatially resolved dating technique using HR-OSL. *Radiation Measurements* **41**, 738-743.

Guerin, G. (2006). Some aspects of phenomenology and kinetics of high temperature thermoluminescence of plagioclase feldspars. *Radiation Measurements* **41**, 936-941.

Hashimoto, T., Fujita, H., Sakaue, H., Nakata, Y., and Nomura, S. (2006). Comparison of accumulated doses in quartz and feldspar extracts from atomic bomb-exposed roof tiles using several luminescence methods. *Radiation Measurements* **41**, 1015-1019.

Huot, S., Buylaert, J. P., and Murray, A. S. (2006). Isothermal thermoluminescence signals from quartz. *Radiation Measurements* **41**, 796-802.

Ige, O. A., Tubosun, I. A., Ogundare, F. O., Mokobia, C. E., and Balogun, F. A. (2006). TL response of muscovite samples from granite pegmatite of Ilesa and Ijero-Ekiti, Southwestern Nigeria. *Radiation Measurements* **41**, 967-970.

Jain, M., Andersen, C. E., Botter-Jensen, L., Murray, A. S., Haack, H., and Bridges, J. C. (2006). Luminescence dating on Mars: OSL characteristics of Martian analogue materials and GCR dosimetry. *Radiation Measurements* **41**, 755-761.

Kalchgruber, R., Blair, M. W., and McKeever, S. W. S. (2006). Dose recovery with plagioclase and pyroxene samples as surrogates for Martian surface sediments. *Radiation Measurements* **41**, 762-767.

Kitis, G., Pagonis, V., and Chen, R. (2006). Comparison of experimental and modelled quartz thermal-activation curves obtained using multiple- and single-aliquot procedures. *Radiation Measurements* **41**, 910-916.

Kiyak, N. G., and Canel, T. (2006). Equivalent dose in quartz from young samples using the SAR protocol and the effect of preheat temperature. *Radiation Measurements* **41**, 917-922.

Klasen, N., Fiebig, M., Preusser, F., and Radtke, U. (2006). Luminescence properties of glaciofluvial sediments from the Bavarian Alpine Foreland. *Radiation Measurements* **41**, 866-870.

Kristianpoller, N., Weiss, D., and Chen, R. (2006). Effects of photostimulation in natural zircon. *Radiation Measurements* **41**, 961-966.

Lahaye, C., Godfrey-Smith, D. I., Guibert, P., and Bechtel, F. (2006). Equivalent thermal history (HE) of ferruginous sandstones based on the thermal activation characteristics of quartz. *Radiation Measurements* **41**, 995-1000.

Lai, Z., and Murray, A. (2006). Red TL of quartz extracted from Chinese loess: Bleachability and saturation dose. *Radiation Measurements* **41**, 836-840.

Li, B., and Li, S.-H. (2006). Correcting for thermal transfer in OSL measurements of young sediment samples. *Radiation Measurements* **41**, 855-861.

Lin, M., Yin, G., Ding, Y., Cui, Y., Chen, K., Wu, C., and Xu, L. (2006). Reliability study on ESR dating of the aluminum center in quartz. *Radiation Measurements* **41**, 1045-1049.

Mayya, Y. S., Morthekai, P., Murari, M. K., and Singhvi, A. K. (2006). Towards quantifying beta microdosimetric effects in single-grain quartz dose distribution. *Radiation Measurements* **41**, 1032-1039.

McKeever, S. W. S., Kalchgruber, R., Blair, M. W., and Deo, S. (2006). Development of methods for in situ dating of martian sediments. *Radiation Measurements* **41**, 750-754.

Mebhah, D., Imatoukene, D., Abdelazziz, F. Z., and Lounis-Mokrani, Z. (2006). Evaluation of trap parameters associated with thermoluminescence peaks in fired quartz. *Radiation Measurements* **41**, 813-818.

Moska, P., and Murray, A. S. (2006). Stability of the quartz fast-component in insensitive samples. *Radiation Measurements* **41**, 878-885.

Ogundare, F. O., Balogun, F. A., and Hussain, L. A. (2006). Evaluation of kinetic parameters of traps in thermoluminescence phosphors. *Radiation Measurements* **41**, 892-896.

Pagonis, V., Chen, R., and Lawless, J. L. (2006). Nonmonotonic dose dependence of OSL intensity due to competition during irradiation and readout. *Radiation Measurements* **41**, 903-909.

Preusser, F., Ramseyer, K., and Schluchter, C. (2006). Characterisation of low OSL intensity quartz from the New Zealand Alps. *Radiation Measurements* **41**, 871-877.

Richter, D., and Temming, H. (2006). Testing heated flint palaeodose protocols using dose recovery procedures. *Radiation Measurements* **41**, 819-825.

Roberts, H. M. (2006). Optical dating of coarse-silt sized quartz from loess: Evaluation of equivalent dose determinations and SAR procedural checks. *Radiation Measurements* **41**, 923-929.

Shimizu, N., Mitamura, N., Takeuchi, A., and Hashimoto, T. (2006). Dependence of radioluminescence on TL-properties in natural quartz. *Radiation Measurements* **41**, 831-835.

Solongo, S., Wagner, G. A., and Galbaatar, T. (2006). The estimation of D_e using the fast and medium components in fired quartz from archaeological site Karakorum, Mongolia. *Radiation Measurements* **41**, 1001-1008.

Tajika, Y., and Hashimoto, T. (2006). Correlation of blue-thermoluminescence (BTL) properties with some impurities in synthetic quartz. *Radiation Measurements* **41**, 809-812.

Takada, M., Tani, A., and Shimada, A. (2006). Preliminary study of the application of natural olivine in Cenozoic dating. *Radiation Measurements* **41**, 982-986.

Takashi, Y., Tomoyuki, T., and Tetsuo, H. (2006). Dependence of luminescence sensitivities of quartz on [alpha]-[beta] phase inversion break temperatures. *Radiation Measurements* **41**, 841-846.

Takeuchi, A., Nagahama, H., and Hashimoto, T. (2006). Surface resetting of thermoluminescence in milled quartz grains. *Radiation Measurements* **41**, 826-830.

Tani, A., Ishikawa, K., and Takeya, K. (2006). Thermal stability of methyl radical in [gamma]-ray irradiated methane hydrate under different pressure from 0.003 to 1 MPa. *Radiation Measurements* **41**, 1040-1044.

Thomsen, K. J., Botter-Jensen, L., Denby, P. M., Moska, P., and Murray, A. S. (2006). Developments in luminescence measurement techniques. *Radiation Measurements* **41**, 768-773.

Tribolo, C., and Stokes, S. (2006). Underestimation of SAR equivalent doses for quartz from West Africa: A dose recovery study. *Radiation Measurements* **41**, 930-935.

Tsirliganis, N., Polymeris, G., Loukou, Z., and Kitis, G. (2006). Anomalous fading of the TL, Blue-SL and IR-SL signals of fluorapatite. *Radiation Measurements* **41**, 954-960.

Tsukamoto, S., Denby, P. M., Murray, A. S., and Botter-Jensen, L. (2006). Time-resolved luminescence from feldspars: New insight into fading. *Radiation Measurements* **41**, 790-795.

Vieillevigne, E., Guibert, P., Rita Zuccarello, A., and Bechtel, F. (2006). The potential of optically stimulated luminescence for medieval building; A case study at Termez, Uzbekistan. *Radiation Measurements* **41**, 991-994.

Visocekas, R., and Guerin, G. (2006). TL dating of feldspars using their far-red emission to deal with anomalous fading. *Radiation Measurements* **41**, 942-947.

Selected papers from 14th International Conference on Solid State Dosimetry held in Yale in 2004

Ankjaergaard, C., Murray, A. S., and Denby, P. M. (2006). Thermal pre-treatment in the OSL dating of quartz: is it necessary? *Radiation Protection Dosimetry* **119,** 470-473.

Baffa, O., Kinoshita, A., Figueiredo, A. M. G., Brunetti, A., and Ginesu, S. (2006). ESR dating of an ancient goat tooth from Nuoro, Sardinia, Italy. *Radiation Protection Dosimetry* **119,** 446-449.

Bernal, R., Souza, D. N., Valerio, M. E. G., Cruz-Vazquez, C., and Barboza-Flores, M. (2006). Optically stimulated luminescence dosimetry performance of natural Brazilian topaz exposed to beta radiation. *Radiation Protection Dosimetry* **119,** 161-163.

Blair, M. W., Yukihara, E. G., and McKeever, S. W. S. (2006). Progress towards a polymineral single-aliquot OSL dating procedure. *Radiation Protection Dosimetry* **119,** 450-453.

Blair, M. W., Yukihara, E. G., and McKeever, S. W. S. (2006). A system to irradiate and measure luminescence at low temperatures. *Radiation Protection Dosimetry* **119,** 454-457.

Buylaert, J. P., Murray, A. S., Huot, S., Vriend, M. G. A., Vandenberghe, D., De Corte, F., and Van den haute, P. (2006). A comparison of quartz OSL and isothermal TL measurements on Chinese loess. *Radiation Protection Dosimetry* **119,** 474-478.

Chen, R., Lo, D., and Lawless, J. L. (2006). Non-monotonic dose dependence of thermoluminescence. *Radiation Protection Dosimetry* **119,** 33-36.

Chernov, V., Paz-Moreno, F., Piters, T. M., and Barboza-Flores, M. (2006). Optical absorption, TL and IRSL of basic plagioclase megacrysts from the pinacate (Sonora, Mexico) quaternary alkalic volcanics. *Radiation Protection Dosimetry* **119,** 233-237.

Correcher, V., Gomez-Ros, J. M., Garcia-Guinea, J., Martin, P. L., and Delgado, A. (2006). Thermal stability of the thermoluminescence trap structure of bentonite. *Radiation Protection Dosimetry* **119,** 176-179.

Goksu, H. Y., and Bailiff, I. K. (2006). Luminescence dosimetry using building materials and personal objects. *Radiation Protection Dosimetry* **119,** 413-420.

Gomez-Ros, J. M., Correcher, V., Garcia-Guinea, J., and Delgado, A. (2006). Evolution of the trapped charge distribution due to trap emptying processes in a natural aluminosilicate. *Radiation Protection Dosimetry* **119,** 93-97.

Gomez-Ros, J. M., Furetta, C., and Correcher, V. (2006). Simple methods to analyse thermoluminescence glow curves assuming arbitrary recombination-retrapping rates. *Radiation Protection Dosimetry* **119,** 339-343.

Guzzo, P. L., Khoury, H. J., Souza, C. P., Souza, A. M., Jr., Schwartz, M. O. E., and Azevedo, W. M. (2006). Defect analysis in natural quartz from Brazilian sites for ionising radiation dosimetry. *Radiation Protection Dosimetry* **119,** 168-171.

Kitis, G., Pagonis, V., Chen, R., and Polymeris, G. (2006). A comprehensive comparative study of the predose effect for three quartz crystals of different origin. *Radiation Protection Dosimetry* **119,** 438-441.

Kristianpoller, N., Weiss, D., and Chen, R. (2006). Optical and dosimetric properties of zircon. *Radiation Protection Dosimetry* **119,** 267-270.

Michael, C. T., and Zacharias, N. (2006). Equivalent dose (palaeodose) estimation in thermoluminescence dating using a single aliquot of polymineral fine grains. *Radiation Protection Dosimetry* **119,** 458-461.

Murray, A. S., and Mohanti, M. (2006). Luminescence dating of the barrier spit at Chilika lake, Orissa, India. *Radiation Protection Dosimetry* **119,** 442-445.

Murthy, K. V. R., Pallavi, S. P., Rahul, G., Patel, Y. S., Sai Prasad, A. S., and Elangovan, D. (2006). Thermoluminescence dosimetric characteristics of beta irradiated salt. *Radiation Protection Dosimetry* **119,** 350-352.

Pagonis, V., Chen, R., and Kitis, G. (2006). Theoretical modelling of experimental diagnostic procedures employed during pre-dose dosimetry of quartz. *Radiation Protection Dosimetry* **119,** 111-114.

Tatumi, S. H., Gozzi, G., Yee, M., de Oliveira, V. I., Sallun, A. E. M., and Suguio, K. (2006). Luminescence dating of Quaternary deposits in geology in Brazil. *Radiation Protection Dosimetry* **119,** 462-469.

van Dijk, J. W. E. (2006). Thermoluminescence glow curve deconvolution and its statistical analysis using the flexibility of spreadsheet programs. *Radiation Protection Dosimetry* **119,** 332-338.

Veronese, I., El-Faramawy, N., Giussani, A., Cantone, M. C., Shishkina, E. A., and Goksu, H. Y. (2006). The use of α-Al_2O_3:C in Risø OSL single grains attachment system for assessing the spatial dose rate distribution due to incorporation of ^{90}Sr in human teeth. *Radiation Protection Dosimetry* **119,** 408-412.

Yamamoto, M., and Tsuchiya, N. (2006). Application of TL as a geochemical sensor. *Radiation Protection Dosimetry* **119,** 119-123.

Letters

Thoughts arising from "Choi, Duller and Wintle: Analysis of quartz LM-OSL curves. *Ancient TL* 24, 9-20 (2006)" by D.J. Huntley

Department of Physics, Simon Fraser University, Burnaby, BC, V5A 1S6, Canada
(Received 2 August 2006)

1) The authors indicate that the linear-modulation (LM) method gives a "more effective and accurate characterization" of each component. There is room for discussion on this matter. LM provides no more information than one obtains using constant excitation. One can readily transform data obtained using constant excitation to that obtained using LM excitation (excitation power increasing linearly with time), or any other time-dependent excitation. The attractive feature of LM excitation is that the emission intensity displays one or more peaks which are much more interesting to look at than a steadily decaying curve, and it may well be easier for the eye to see different components. Nevertheless any analysis of the data taken either way should produce the same results.

Using constant excitation power takes less measurement time and the background is expected to be constant (unless the emission from the diodes is changing), thus leading to a simpler experiment. The mathematical transformation is readily accomplished with a computer and could be performed while the data are collected.

The above comments are predicated on the assumption that the emission per unit incident flux is a function of the total incident flux to that point, and not on how that incident flux was distributed in time. A special case of this is when the emission arises from a sum of several 1st-order decays. The assumption will not be valid if the excitation cross-section depends on excitation power, which seems unlikely to be significant. The assumption will not be valid if there is significant retrapping and re-excitation on the time scale of the measurement; this is a substantial concern. One method of detecting this is to switch the excitation off, wait, and switch it on again; if the emission intensity is different when the excitation is switched on then the assumption is not valid. An example of this can be found in Aitken and Smith (1988, Figure 2). An alternative way of testing the assumption is to analyze LM data and constant-excitation data for the same sample; if the results are different then the assumption is not valid; Kuhns et al. (2000) provide an example of this.

2) Figure 1a showing background data that is not increasing linearly with excitation power is very worrying, as the authors recognize. They suggest that it arises from the emission spectrum of the diodes changing as the power is increased, with a resulting change in the portion of the scattered excitation photons passing through the filters. If this is true then there will also be a significant change in the excitation cross section because that is exponentially dependent on the photon energy (e.g. Huntley et al., 1996). This may well be sufficient to invalidate the analyses.

3) There is a problem I have mentioned before in Ancient TL in connection with using blue LEDs. This is Raman scattering of excitation photons from the sample, the sample holder, and from anything else that the incident photons may scatter from into the detector. The closer in energy that the excitation photons are to the pass band of the measuring system the worse this problem will be. As well, Raman scattering increases exponentially with sample temperature and it is expected to be sample dependent. I have seen nothing in any paper addressing this issue. I expect it to be significant for the usual measurements on quartz. For this reason I favour the use of green LEDs until someone proves that Raman scattering of blue photons by quartz is not significant. Examples of Raman scattering from feldspars and zircons can be found in Huntley et al. (1989) and Godfrey-Smith et al. (1989) respectively.

References

Aitken, M.J. and Smith, B.W. (1988) Optical dating: recuperation after bleaching. *Quaternary Science Reviews* **7**, 387-393.

Godfrey-Smith, D.I., McMullan, W.G., Huntley, D.J. and Thewalt, M.L.W. (1989) Time-dependent recombination luminescence spectra arising from optical ejection of trapped charges in zircons. *Journal of Luminescence* **44**, 47-58.

Huntley, D.J., McMullan, W.G., Godfrey-Smith, D.I. and Thewalt, M.L.W. (1989) Time-dependent recombination spectra arising from optical

ejection of trapped charges in feldspars. *Journal of Luminescence* **44**, 41-46.

Huntley, D.J., Short, M.A. and Dunphy, K. (1996) Deep traps in quartz and their use for optical dating. *Canadian Journal of Physics* **74**, 81-91.

Kuhns, C.K., Agersnap Larsen, N. and McKeever, S.W.S. (2000) Characteristics of LM-OSL from several different types of quartz. *Radiation Measurements* **32**, 413-418.

Conference Announcement

UK Luminescence and ESR Meeting

Department of Geography
University of Sheffield

The University Of Sheffield.

12-14th September 2007

The annual UK Luminescence and ESR dating research meeting will be held at the University of Sheffield from the 12-14th September 2007. This meeting will be of interest to luminescence dating specialists, Quaternary geologists, archaeologists, dosimetric scientists and some physics researchers by providing an opportunity to discuss the latest research in trapped charge dating and related work. Presentations covering basic physics, methodological issues and the application of these techniques are all welcome. The meeting will consist of both oral and poster presentations, and presentations by research students are especially encouraged.

For further information send an e-mail to: Luminescence@sheffield.ac.uk or visit the University of Sheffield Geography department website at http://www.shef.ac.uk/geography/

Notice

It is with sadness that we note the passing of Professor W.F. Hornyak on 17 August 2006.

Bill had a career as a nuclear physicist, but in his later years he was interested in aspects of nuclear science applied to archaeology. He set up a TL laboratory in the Physics Department of the University of Maryland and established a long-standing working relationship with Professor Alan Franklin, publishing several papers on TL and OSL of quartz.